JOURNAL OF GEOPHYSICAL RESEARCH, VOL. 101, NO. D6, PAGES 9603–9620, APRIL 30, 1996

Validation of CLAES $ClONO_2$ measurements

J. L. Mergenthaler,[1] J. B. Kumer,[1] A. E. Roche,[1] R. W. Nightingale,[1] J. F. Potter,[1]
J. C. Gille,[2] S. T. Massie,[2] P. L. Bailey,[2] D. Edwards,[2] P. S. Connell,[3]
D. E. Kinnison,[3] M. R. Gunson,[4] M. C. Abrams,[4] G. C. Toon,[4] B. Sen,[4]
J.-F. Blavier,[4] D. G. Murcray,[5] F. J. Murcray,[5] and A. Goldman[5]

Abstract. The cryogenic limb array etalon spectrometer (CLAES) aboard the Upper Atmosphere Research Satellite has made extensive measurements of thermal infrared radiation from the Earth's limb from which vertical concentration profiles of several stratospheric gases and multiwavelength aerosol absorption coefficients have been retrieved for the period from January 9, 1992, to May 5, 1993. This work examines stratospheric $ClONO_2$ concentrations from the current calibration and retrieval software which are designated version 7 data. These data provide the first near-global view of this stratospheric species. This work evaluates data quality through (1) an analysis of estimated uncertainties and biases in the remote sensing process, (2) comparison with calculations using a two-dimensional chemical model, (3) comparison with correlative data, and (4) an examination of various known limitations. The precision of CLAES $ClONO_2$ volume mixing ratio retrievals are within 15% in the range ($10 < P < 50$ mbar). The upper limit on estimated systematic error is 28% in the range ($10 < P < 100$ mbar) based on studies of error sources in midlatitude retrievals. The global distribution of $ClONO_2$ computed with the Lawrence Livermore National Laboratory two-dimensional stratospheric chemistry model and the CLAES measurements agree qualitatively. However, above the profile peak the calculated concentration frequently exceeds the measurement. CLAES and ATMOS measurements show relatively good midlatitude agreement, suggesting that the major source of discrepancy is in the model. A possible explanation in terms of a missing reaction $ClO + OH \rightarrow HCl + O_2$ is suggested. Also, the $ClONO_2$ diurnal cycle constructed from more than 30 days of CLAES data agrees well with the model. The CLAES $ClONO_2$ data differ from correlative data acquired on flights of the shuttle-based ATMOS and balloon-borne instruments by less than 25% on the average in the $10 < P < 50$ mbar range. At altitudes above 10 mbar the CLAES measurement is biased low with respect to correlative measurements. This discrepancy at high altitudes is consistent with the analysis showing a large increase of systematic errors above 10 mbar. Heavy tropical volcanic aerosol from the Mount Pinatubo eruption in June 1991 apparently interfered with $ClONO_2$ retrievals in the period before July 1992, causing anomalous peaks in the $20 < P < 30$ mbar region accompanied by very small concentrations below the peak ($P > 30$ mbar). A similar effect associated with thick polar stratospheric clouds is identified. Overall, this validation study indicates that the majority of these data are of good quality and should be very useful in quantitative and qualitative chemical studies of the stratosphere.

Introduction

The stratospheric chlorine nitrate, $ClONO_2$, is of interest since it is a temporary reservoir of chlorine which couples the NO_x and ClO_x cycles. It plays an important role in the ozone budget for the lower stratosphere in "normal" gas phase chemistry and the heterogeneous chemistry of the polar winter and possibly volcanically perturbed periods. *Rowland et al.* [1976a, b] pointed out the possible existence of $ClONO_2$ in the stratosphere and gave some formation and destruction reactions. They also presented a theoretical profile relative to the inert chlorine reservoir, HCl, and discussed the possibility of detecting $ClONO_2$ in the stratosphere through its infrared absorption bands. *Murcray et al.* [1979] subsequently reported the first detection of chlorine nitrate in the stratosphere from the absorption of solar radiation at 1292 cm^{-1} measured with a balloon-borne Fourier transform spectrometer (FTS). Later, *Rinsland et al.* [1985] identified the $ClONO_2$ ν_4 Q branch at 780.2 cm^{-1} in atmospheric spectra. *Zander et al.* [1986] reported the first multiple band identification of $ClONO_2$ with the atmospheric trace molecule spectroscopy (ATMOS) instrument from the shuttle-based Spacelab 3. *Massie et al.* [1987] reported the first thermal emission measurement of stratospheric $ClONO_2$ using the 780.2 cm^{-1} and the 809 cm^{-1} bands. During this period the Antarctic "ozone hole" was revealed [*Farman et al.*, 1985] and largely explained through

[1]Lockheed Palo Alto Research Laboratory, Palo Alto, California.
[2]National Center for Atmospheric Research, Boulder, Colorado.
[3]Lawrence Livermore National Laboratory, Livermore, California.
[4]Jet Propulsion Laboratory, Pasadena, California.
[5]University of Denver, Denver, Colorado.

Paper number 96JD00449.
0148-0227/96/96JD-00449$05.00

Table 1. Spectral Sampling Positions Used for O_3, $ClONO_2$, and Aerosol Retrieval

Spectral Position	Wavenumber, cm^{-1}	Spectral Feature
(1)	779.18	minimum
(2)	779.48	O_3 peak
(3)	779.83	minimum
(4)	780.07	O_3 peak
(5)	780.21	$ClONO_2$ peak
(6)	780.35	O_3 peak
(7)	780.50	$CO_2 + O_3$

denitrification by sedimenting polar stratospheric clouds (PSCs) and heterogeneous reactions [*Solomon*, 1990], which release chlorine from the HCl and $ClONO_2$ reservoirs. With the realization of the importance of heterogeneous chemistry, concerns have been raised about ozone depletion via reactions on sulfate aerosol unlocking chlorine from the chlorine nitrate reservoir [*Hoffman and Solomon*, 1989] and [*Prather*, 1992]. Recently, the question of a catalytic ozone destruction cycle involving the regeneration of $ClONO_2$ has been proposed [*Toumi et al.*, 1993].

The mission of the Upper Atmosphere Research Satellite (UARS) is discussed by *Reber et al.* [1993]. The cryogenic limb array etalon spectrometer (CLAES) aboard UARS is the first instrument to provide three-dimensional fields of $ClONO_2$ sampling over 77% of the globe daily. Designed for an 18-month on-orbit lifetime, CLAES actually operated for 19 months, acquiring 470 days of data. To date, 388 of these days (between January 9, 1992, and May 5, 1993) have been processed using version 7 data processing software. A typical daily file contains over 1200 altitude profiles of the $ClONO_2$ volume mixing ratio (VMR). Before the UARS launch, fewer than 10 $ClONO_2$ profile measurements were reported in the literature although several valuable column measurements were published as part of polar campaigns by *Farmer et al.* [1987a], *Toon et al.* [1989], and *Coffey et al.* [1989].

CLAES measurements are the first multiseason, near-global data set for this important stratospheric species. The purpose of this paper is to present an assessment of the quality of the CLAES $ClONO_2$ data.

The remainder of this paper is divided into five sections. The first section provides a brief description of the CLAES instrument and the measurement technique and also presents an analysis of expected precision and accuracy. The second compares measurements with theoretical calculations from the Lawrence Livermore National Laboratory two-dimensional LLNL-2D atmospheric chemistry model. The third presents comparisons with correlative data. The fourth examines data artifacts. The fifth section presents a summary and conclusions.

Observations and Error Estimates

Vertical concentration profiles of several stratospheric gases, temperature, and multiwavelength aerosol absorption coefficients are derived from CLAES measurements of atmospheric infrared emission in a limb-viewing mode. The instrument and measurement technique are described in detail by *Roche et al.* [1993a]. In brief, after entering the instrument through a cooled telescope, the earthlimb thermal emission passes through one of four Fabry-Perot etalons mounted on a paddle wheel and one of nine blocking filters mounted in a wheel. Each filter isolates a spectral channel $\approx 10\ cm^{-1}$ wide that includes features of one or more target species and is matched to a specific etalon according to the frequency of its transmission peak. The etalon provides a spectral resolution of 0.2–0.65 cm^{-1} and a method of spectral scanning by tilting the paddle wheel. The spectrally filtered radiation is imaged on an array of 20 detectors. Each detector integrates radiance from a 2.5 km vertical footprint on the Earth's limb, so the entire array provides an altitude coverage of 50 km, normally 10 to 60 km. During normal operation, which occupied about 94% of viewing time, one profile of each target species was acquired in each 65.536-s period which is referred to as an engineering major frame (EMAF). Each EMAF corresponds to tangent point movement of about 500 km.

The UARS 57° inclination orbit was chosen to obtain wide geographical coverage and to provide measurements through the diurnal cycle. The spacecraft is yawed 180° every 36 days, switching coverage from 34°N–80°S to 80°S–34°N or vice versa. During ascending (northward moving) and descending (southward moving) halves of the orbit, the instrument samples at local solar times (LSTs) separated by up to 12 hours depending on latitude. The orbit precesses 5° per day relative to the Sun, providing nearly full midlatitude diurnal coverage in a yaw cycle.

The instrument telescope aperture door was closed for approximately 5 days during each spacecraft yaw to protect against direct solar loading on the stored cryogens via the telescope and baffles. A high emissivity blackbody calibration source on the inside of the telescope door was used for end-to-end radiometric calibration during the yaw-maneuver door closings. The door was also closed for 1–2 days halfway between the yaws (roughly every 2 weeks) for additional radiometric calibration.

The filter used to retrieve chlorine nitrate transmits from approximately 775 to 785 cm^{-1} and has a peak near 780 cm^{-1} with a full width at half maximum (FWHM) transmission of $\approx 2.0\ cm^{-1}$. The silicon etalon used in this region has a transmission order separation or free-spectral-range (FSR) of 5.28 cm^{-1}. For the routine spectral sampling positions this allows significant radiance contributions from one etalon transmission order near the filter center and small sidelobes located an FSR to either side. The effective FWHM of the etalon spectral transmission function is 0.25 cm^{-1} at normal incidence, broadening to 0.4 cm^{-1} at a 23° tilt angle. Most of the atmospheric emission features measured for $ClONO_2$ retrieval are sampled with a value of 0.32 cm^{-1} near a 17° tilt.

The number of etalon positions sampled in each filter region during normal operation is limited by the necessity to obtain an entire measurement cycle in an EMAF. This filter is sampled by 21 etalon positions or seven groups of three microsteps. Each group of three positions is in the neighborhood of a distinguishing feature in the atmospheric spectrum, for example the peak of an ozone feature or a local minimum. The wavenumber corresponding to a specific etalon tilt angle varies with detector due to spectral dispersion along the vertical extent of the array ($\approx 0.03\ cm^{-1}$ difference from the center to end detectors). Interpolation within the three-position cluster allows one to obtain the same spectral frequency at all 20 detectors. This is done for seven frequencies which are shown in Table 1 along with their corresponding spectral features.

Figure 1 shows a CLAES spectrum in the $ClONO_2/O_3$ region that was acquired in the region of high $ClONO_2$ concentration occurring near the end of the Antarctic winter in the

"collar region" of the polar vortex. The spectrum was acquired using a special continuous scan mode designed for spectral calibration. In this mode the entire EMAF, normally used to sample all spectral regions, is devoted to scanning a single filter with small angular steps of the etalon. Figure 1 also shows the seven operational sampling positions and the spectra of the primary emitters in this channel as computed with the line-by-line spectral radiance code, FASCODE3 [*Clough et al.*, 1988]. These emitters include O_3 (lines from the [010-000] band centered at 700.93 cm^{-1}), CO_2 (lines from the [11101-10002] band centered at 791.45 cm^{-1}), $ClONO_2$ (ν_4 band at 780.21 cm^{-1}), aerosol, and the minor contributor HNO_3. A least squares fit of the sum of these contributions to the CLAES data shows that all major emission features have been taken into account.

Another example of CLAES continuous spectra is shown in Figure 2 with data acquired on January 9, 1992, in the midlatitudes. Scans through the region of significant $ClONO_2$ contribution show that the radiance measurements contain substantial contributions from aerosol, O_3, $ClONO_2$, and CO_2 whose relative magnitudes vary considerably with altitude. At the time the atmosphere was heavily laden with aerosol from the Mount Pinatubo eruptions resulting in the large continuum component which decays rapidly with increasing altitude.

The retrieval problem is broken into an equivalent of a single emitter and single-channel problem for each constituent by using a linear least squares approach fitting calculated to observed radiance. Next, a method similar to the Newtonian iterative algorithm described by *Rodgers* [1976, equation (99), p. 621] is used for error estimation and retrieval of each constituent. For production data processing, the method requires a computationally efficient algorithm for calculation of radiance profiles. The model described by *Marshall et al.* [1994] is used for this purpose. The method employs an initial guess species profile provided by the UARS prelaunch climatology developed by R. R. Seals and D. J. Wuebbles (see *Kumer et al.* [1993] for a description). The pressure and temperature profiles for radiance computations are retrieved in an adjacent spectral region centered at 790 cm^{-1}. In the $ClONO_2$ region

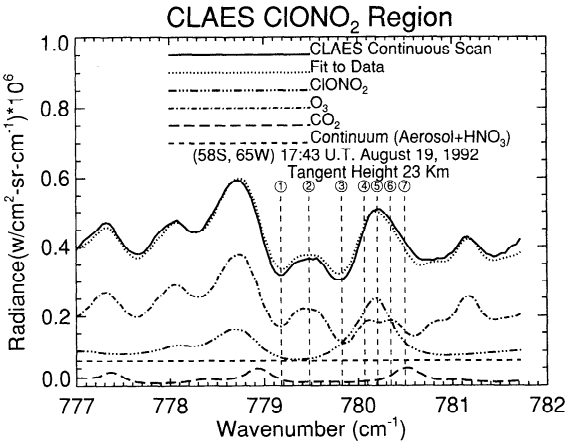

Figure 1. A continuous scan of the $ClONO_2/O_3$ spectral region. Contributions to the radiance from O_3, $ClONO_2$, CO_2, and a continuum (aerosol + HNO_3) are shown along with a least squares fit to the data. The seven operational science mode sampling positions are indicated. This example is from the edge of Antarctic winter vortex where a "collar" of high $ClONO_2$ and HNO_3 appears. (See *Roche et al.* [1994], Figure 11, for a global view of $ClONO_2$ volume mixing ratio (VMR).)

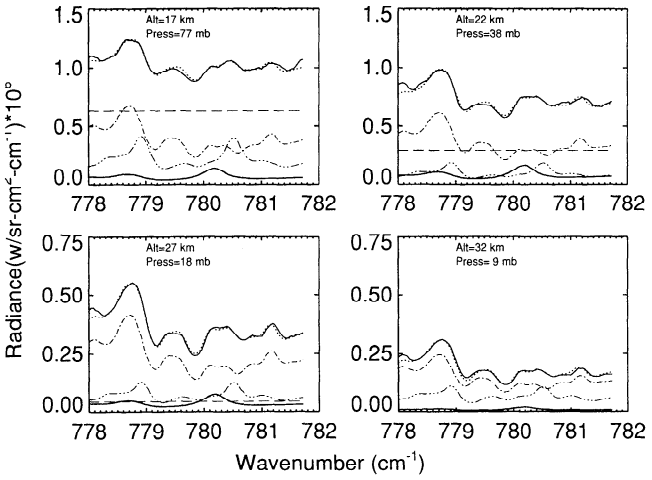

Figure 2. The progression in height of cryogenic limb array etalon spectrometer (CLAES) continuous scan spectra and species radiance contributions through the region of significant $ClONO_2$ contribution. The data were acquired on January 9, 1992, at 37°N 51°W at 0424 UT during a period of heavy aerosol perturbation. The solid line is the CLAES data, the data (top solid line), and a least squares fit (dotted line) along with radiance components from $ClONO_2$ (bottom solid line), the O_3 (dashed-dotted), CO_2 (dashed-three dotted line), and aerosol (dashed) are shown.

the computed radiance due to the CO_2 component is subtracted from the total radiance based on a constant mixing ratio of 350 parts per million by volume (ppmv). The inversion solution yields O_3, $ClONO_2$, and aerosol concentrations which reproduce the remaining spectral radiance in accordance with the fitting procedure. Four iterations, the number used in the version 7 software, are sufficient to achieve a solution. The retrieval and algorithmic error estimates are discussed in further detail by *Kumer et al.* [this issue]. The quality of the ozone mixing ratio and aerosol extinction coefficients that are retrieved simultaneously with $ClONO_2$ are treated by *Bailey et al.* [this issue] and *Massie et al.* [this issue], respectively.

On a global scale our studies have shown the $ClONO_2$ solution to have little sensitivity to the initial guess. Illustrating this, Figure 3 compares two initial guess profiles and corresponding $ClONO_2$ retrievals for November 25, 1992, at 46°S

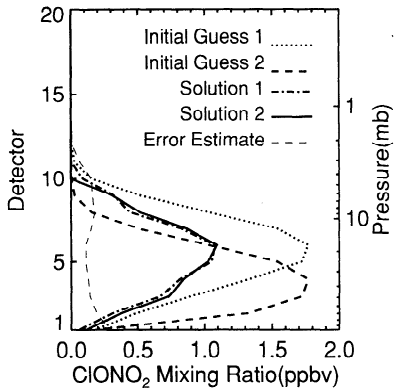

Figure 3. Two different "initial guess" $ClONO_2$ VMR vertical profiles and the results from four iterations of the CLAES version 7 processing software.

Table 2. Systematic Error Estimates (% $ClONO_2$ Volume Mixing Ratio)

Error Source	Pressure, mbar				
	100	46	20	10	4.6
Radiometric calibration	1.0	1.1	1.2	2.3	2.4
Spectral calibration	0.6	0.6	0.6	0.6	0.6
Spectral response function	2.7	3.0	3.0	3.0	3.0
Array spectral dispersion	0.9	1.2	0.9	0.3	0.1
Detector spatial response	0.5	0.3	1.3	1.9	0.9
Optical cross talk	0.2	0.2	0.2	0.4	1.0
Retrieved temperature	4.5	5.0	4.8	4.8	3.5
Forward radiance	0.9	1.0	1.0	1.0	1.0
$ClONO_2$ spectral parameters	20.1	20.0	20.2	20.4	21.5
CO_2 component	4.6	2.3	2.4	7.5	>100.0
O_3 component	11.0	8.5	8.2	17.0	>100
rss of errors	24	23	23	28	>100

249°E. The solutions differ by less than the algorithmic error estimate, shown as a dashed line.

Estimation of Experiment Systematic and Random Errors

The approach to estimating errors in retrieved $ClONO_2$ VMR was to multiply estimated radiance errors by an altitude dependent ratio found empirically by determining the sensitivity of the retrieval to changes in the input radiance. Estimated errors in the vertical location of the detector footprints at the earthlimb were translated into approximate VMR errors using midlatitude retrieved $ClONO_2$ vertical profiles. Estimates are provided below for radiance errors and the resulting systematic errors in retrieved $ClONO_2$ VMR are summarized in Table 2 and random errors in Table 3.

Systematic Errors

Radiometric calibration. Atmospheric radiances are calibrated using the onboard blackbody calibration source (OBCS). Determination of spectral radiance from this source involves biases in the OBCS temperature as determined from five platinum resistance thermometers (PRTs), uncertainties in the knowledge of the absolute emissivity, offsets in the electronic zero-photon level, uncertainty in foreoptics thermal emission, and the use of a detector "characteristic responsivity curve" fitting technique to provide responsivities for low atmospheric radiances. The design and prelaunch characterization of the OBCS have been discussed by *Sterritt et al.* [1990]. Temperature and emissivity uncertainties in the 780 cm^{-1} $ClONO_2$ spectral position amount to approximately 1% rms radiance error. The other uncertainties are significant under high-altitude, low-radiance conditions. The square root of the sum of the squares (rss) of all systematic radiometric calibration radiance uncertainties were estimated to be in the range 1.0 to 2.4% between 100 and 4.6 mbar.

Instrument characterization. This includes (1) spectral calibration, (2) spectral response function, (3) spectral dispersion along the array vertical extent, (4) detector spatial responsivity, and (5) optics out-of-field stray light rejection and in-field scattering (optical cross talk). *James et al.* [1990] discuss the design and prelaunch characterization of the CLAES solid Fabry-Perot etalons. *Mergenthaler et al.* [1990], *Kumer et al.* [1990], and *Mergenthaler et al.* [1993] discuss aspects of the design and prelaunch characterization of the filters. Information on the absolute wavelength calibration and the effective spectral transmission function were also deduced from on-orbit spectral scans of specific emission features. Limits on off-axis and in-field scattering were deduced on orbit from high-altitude and "cold space" radiance measurements.

We estimated an uncertainty of 0.01 cm^{-1}, both in the absolute spectral calibration and in the width of the spectral response function. The spectral calibration error results in a relatively small radiance error of 0.6%. The uncertainty in the spectral function, however, represents a 3.1% error in the nominal 0.32 cm^{-1} width of the $ClONO_2$ etalon function. The error has some covariance between the measurement of atmospheric spectra and the measurement of the continuumlike radiance from the OCBS, especially emitters such as aerosol and $ClONO_2$ and in the wings of overlapping lines. This would tend to reduce the effective radiance error associated with the spectral function uncertainty for continuum emitters. However, for the purposes of comparing estimated systematic error with that inferred from correlative measurements, the maximum radiance error of 3% was used.

Array dispersion effects contribute less than 1.2% radiance error, and detector uniformity contributes less than 1.3% at altitudes below about 8 mbar. Responsivity changes contribute less than 2% radiance error. In the future this error can be reduced. Optical cross talk contributes less than 1% from 100 to 4.6 mbar. The rss of all instrument characterization radiance uncertainties was estimated to be in the range 3.2 to 7.6% between 100 and 4.6 mbar.

Atmospheric temperature determination. Any systematic error in the retrieval of atmospheric temperature will appear in the forward radiance model as an error in the calculation of the $ClONO_2$ line radiances as well as the radiance of interfering

Table 3. Theoretical Random Error Estimates (% $ClONO_2$ Volume Mixing Ratio)

Error Source	Pressure, mbar				
	100	46	20	10	4.6
Radiometric calibration	23	5	2	2	1
Spectral positioning	21	5	2	2	1
Electronics noise	21	4	2	7	34
Horizontal gradients	20	5	2	2	1
Vertical smear	17	2	3	4	1
Retrieved temperature	40	9	3	3	1
rss-theoretical precision	61	13	6.4	9	34

gases. The sensitivity of the radiance to temperature depends on the transition frequency, the lower state energy of the line transition involved and on the mean atmospheric temperature at the measurement altitude. Temperature sensitivities for calculated $ClONO_2$ radiances in the stratosphere are of the order of 2–3% per degree K. CLAES-retrieved systematic temperature errors vary from about 1.9 to 2.3 K in the 100- to 4.6-mbar range [*Gille et al.*, this issue], which result in $ClONO_2$ radiance errors between 5 and 3.5% from 100 to 4.6 mbar.

Forward radiance model. The evaluation of uncertainties in the forward radiance model primarily involves radiative transfer approximations, treatment of line overlap and mixing, and calculation of EGA table coefficients. Radiance errors of 1% were estimated by comparing the forward model results with rigorous line-by-line code calculations [*Gordley et al.*, 1994].

Spectral parameters. Errors in the calculated radiance used in the retrieval can be caused by errors in the spectral parameters that characterize atmospheric molecular emission. These include errors in the strengths, positions, and shapes of molecular absorption lines as well as their pressure and temperature dependence. Because of lack of individual line data for $ClONO_2$, which is a heavy molecule with very high absorption line density, its emission was characterized by the absorption cross-section measurements at 213°K from *Ballard et al.* [1988] as given by IIITRAN '92 [*Rothman et al.*, 1992]. Through the examination of the retrieval products from test versions we found that a modification of the $ClONO_2$ radiance component reduced the number of anomalous aerosol and ozone profiles occurring in very cold conditions. The resulting profiles became more consistent with retrieval products from the adjacent 790 cm^{-1} region and other data sources. We used this modification in version 7 data processing. It consists of reducing the limb radiance component based on the *Ballard et al.* [1988] cross sections by 50% in the three low wavenumber spectral positions, positions 1 through 3 in Table 1. In these calculations the $ClONO_2$ radiance component is directly proportional to filter-convolved cross sections since no pressure or temperature dependence is used and $ClONO_2$ is optically thin. Therefore this modification is equivalent to using cross sections with a lower continuum on the low wavenumber side of the Q branch.

Recent evidence tends to vindicate this modification. New $ClONO_2$ line parameters have been produced [*Goldman et al.*, 1994] and used in ATMOS retrievals which show much less radiance in the short wavenumber wing of the Q branch and achieve an improved fit to high-resolution atmospheric data [*Rinsland et al.*, 1994]. Figure 4 compares $ClONO_2$ relative spectral radiance for a uniform path at 213°K computed from the cross sections and the new line list using the GENL2 [*Edwards*, 1992] line-by-line spectral radiance code. The CLAES modification is also shown and appears to conform closely with the radiance component computed from the line parameters. Therefore the modification appears to be within the level of uncertainty currently associated with $ClONO_2$ parameters used in the literature. The difference in retrieved $ClONO_2$ from modified and unmodified cross sections is 10–15% and lies within the overall uncertainty attributed to $ClONO_2$ line parameters in the analysis of systematic errors.

For version 7, temperature dependence of the $ClONO_2$ cross sections has not been taken into account. As shown in Figure 8 of *Ballard et al.* [1988], the Q branch narrows and intensifies with lowering temperature. The peak absorption

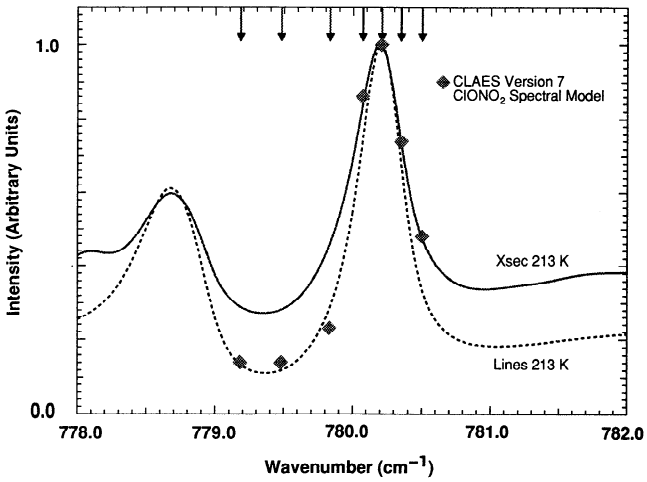

Figure 4. Comparison of $ClONO_2$ spectral radiance models: (1) computed from the 213° K absorption cross sections of *Ballard et al.* [1988], (2) the spectral line list of *Goldman et al.* [1994], and (3) the CLAES version 7 $ClONO_2$ spectral model. The CLAES sampling positions are indicated at the top by arrows.

changes by about 50% with temperature changes from 213°K to 296°K. At CLAES resolution, 0.32 cm^{-1} (compared with Ballard's 0.02 cm^{-1}), the Q-branch peak is smoothed reducing the 296°–213°K difference to 25%. The neglect of the temperature dependence in the $ClONO_2$ spectral parameters is estimated to produce bias errors of 0.33%/°K for temperature excursions away from 213°K with low bias for high temperatures and vice versa. In the near future, line parameters will be available with additional $ClONO_2$ hot bands that contribute in this region. At that time, the temperature dependence in the forward model spectroscopy will be handled explicitly. For $ClONO_2$ the single biggest error is associated with spectral parameter uncertainties.

The spectral parameters for the interfering gases CO_2 and O_3 are from HITRAN '92. The absolute line positions are known to better than 0.001 cm^{-1}. The absolute intensities of the CO_2 and O_3 lines are known to better than 3 and 5%, respectively.

The systematic error in CO_2 radiance has been estimated at 9% based on systematic uncertainties in temperature and line strength. It is the relative shape of the O_3 radiance component that is most important for the $ClONO_2$ retrieval. Uncertainties in it depend on the knowledge of relative line strengths in HITRAN '92, instrument spectral response, and temperature. This uncertainty has been estimated by perturbing the O_3 component by 2% in sampling positions 1–3 relative to positions 4–7. These studies show that $ClONO_2$ retrieval uncertainties from interfering gases begin to dominate the error budget at the high altitude and approach 100% at about 6 mbar for the midlatitude case considered. Results for other levels are listed in Table 2.

Aerosol effects. Historically high levels of aerosol were present for nearly all CLAES measurements. It appears as a continuum component which is usually handled relatively easily by the retrieval algorithm. However, there are situations where the data must be viewed with caution. The error analysis in Table 2 pertains to a midlatitude atmosphere. Very heavy aerosol loading such as Antarctic winter PSCs or the heavy

Mount Pinatubo aerosol in the tropics early in the mission appears to degrade the retrieval in two ways. First, spectral contrast and sensitivity to the tangent point $ClONO_2$ concentration are diminished when the aerosol optical depth through the limb approaches unity. The algorithmic error estimate takes this into account and expands appropriately with increasing aerosol.

The second effect associated with thick aerosol is an apparent distortion of the spectrum measured on the detector just at the top of a very intense PSC or thick tropical aerosol clouds in the region of a very steep radiance gradient. The result is an enhancement in the $ClONO_2$ VMR. Recall from Figure 2 that there are CO_2 emission features in the $ClONO_2$ spectral region. These can be used as a standard to test the quality of constituent retrieval in this region. A consistency check can be performed by comparing magnitude of the CO_2 component that best fits the measured spectrum to that computed from the retrieved temperature, pressure, and known CO_2 mixing ratio. The agreement is usually quite good, well within calculated uncertainties. But larger discrepancies develop in regions of high-radiance gradient and these are coincident with the elevated $ClONO_2$ VMR values in question. The tropical data contaminated by both effects in the early part of the mission are nearly coincident with the region of aerosol extinction greater than 10^{-3}/km shown in Figure 1a of *Roche et al.* [1994]. We give examples of problems in the data set below in the Known Artifacts section.

Random Error Sources

Radiometric calibration. The main contributors to random error in the onboard calibration process involve the repeatability of the PRTs and associated electronics. These uncertainties in the 780.2 cm^{-1} $ClONO_2$ spectral position amount to approximately 1.1% rms radiance error at the OBCS coldest temperature of 160°K. This is expected to be an upper limit for this error.

Instrument effects. The primary instrument contributors to random errors in the measured radiances involve repeatability in the angular (i.e., spectral) positioning of the Fabry-Perot etalons and electronics noise which includes detector and signal processing noise.

Prelaunch measurements of the angular repeatability showed it to be better than 0.03° which corresponds to 0.01 cm^{-1} in spectral precision. A similar value was inferred from observations of scatter in the shape of the on-orbit spectral modulation curves obtained during OBCS calibrations. For the 780.2 cm^{-1} $ClONO_2$ spectral position this results in a random spectral positioning error of less than 1% in the measurement of atmospheric radiances.

Electronic noise is characterized as the noise equivalent spectral radiance (NESR) in units of $W/(cm^2\ sr\ cm^{-1})$. This is defined as the input spectral radiance at the instrument aperture required to give an output (counts, volts) equal to the system noise for a specific integration time. The NESR has a specific value for each of the 20 CLAES detectors and 9 spectral channels and also for the specific spectral positions within a particular channel. The best measure of the effective NESR is obtained by looking at the variance of a large number of operational science mode ("mode 1") spectral profiles obtained when the instrument was rolled up to look high above the atmosphere into a region of very low radiance. Using the roll-up mode 1 radiance ensures that the identical spectral positions, dwell times, and integration times, are obtained as those used when viewing the atmosphere. Further, these roll-up radiances are conditioned in an identical manner to those used in the retrieval of atmospheric parameters, particularly with respect to the reduction of a quasi-sinusoidal low-frequency artifact ("ripple") seen in the electronics dark noise output. These data are largely insensitive to spectral positioning error because the only radiance present is a small continuum from telescope emission. For the seven spectral positions used in the retrieval of species in the 780 cm^{-1} channel the array average NESR obtained from roll-up data lies between 4.6 and 6.0 $\times$ 10^{-10} $W/(cm^2\ sr\ cm^{-1})$. The higher value was used in this discussion. The photon noise term drops below the instrument NESR at altitudes above 10 mbar.

Horizontal gradients. The version 7 processing software models the distribution of the constituents in the stratosphere as uniform spherical shells. Horizontal temperature gradients are treated by a two-step process. Line-of-sight (LOS) temperature gradients from the NMC analysis are initially used in the forward radiance computation. After making global temperature retrievals on this basis, the measurements are mapped and provide global line-of-sight temperature gradients for a second and final global temperature retrieval similar to the method used in LIMS temperature retrievals [*Gille et al.*, 1984].

Real differences in gas or aerosol concentration in a constant altitude atmospheric layer intersecting the LOS on either side of the tangent point can give rise to errors. For $ClONO_2$, significant radiance contributions can be spread for 500 km on either side of the tangent point along the line of sight. The spatial distribution spreads with lowering tangent viewing altitude. Its width, and therefore the potential for sensitivity to horizontal gradients, depends on the temperature and $ClONO_2$ distribution as well as the tangent height altitude. Estimated errors for midlatitude conditions are listed Table 3. It is difficult to characterize all viewing scenarios; however, the estimates in Table 3, which correspond to 1% radiance error, should reasonably represent midlatitude gradients in $ClONO_2$ concentrations, including diurnal cycle differences along the CLAES LOS. The errors due to horizontal gradients near the polar vortex edge could increase by a factor of 3–4.

Vertical smear. During observations a combination of random errors in the positioning of the limb acquisition and adjustment mirror (LAAM) and spacecraft jitter due to array thermal snap results in a vertical jitter of approximately 100 m. The resulting error in mixing ratio will be dependent on the scale height of the species whose line radiances are being observed. For the CLAES $ClONO_2$ 780.2 cm^{-1} spectral position the random VMR error associated with vertical smear has the values listed in Table 3 which vary from 17 to 1% in the 100- to 4.6-mbar range.

Atmospheric temperature determination. Random errors in CLAES-retrieved temperature vary from about 0.7° to 0.9°K in the 100- to 4.6-mbar range [*Gille et al.*, this issue]. This results in $ClONO_2$ radiance errors between 1.9 and 1.4% from 100 to 4.6 mbar.

Table 3 provides estimates of the percent random error in the $ClONO_2$ VMR from these various effects for five pressure levels. Random errors in the retrieved temperature contribute the most to the estimated RSS errors except at 4.6 and 10 mbar where instrument noise dominates. The large drop in rss error from 100 to 46 mbar reflects the much greater sensitivity of the retrieval algorithm to radiance errors on the lowest-pointed detectors, as compared with detectors at even moderately higher tangent point altitudes.

Measured Precision, Theoretical Precision and Algorithmic Error Estimates

A measured precision of the CLAES retrievals was estimated by the average of the difference of VMR profiles measured where the instrument tangent point passes the same location on ascending and descending halves of two contiguous orbits. The condition regularly occurs near the turnaround points at 34°N and 80°S, or 80°N and 34°S, depending upon the spacecraft yaw direction. The colocation of paired CLAES profiles is within 96.4 min, ±1° of latitude and ±2° of longitude. Furthermore, the periods, picked to minimize atmospheric variations due to large-scale dynamics and nighttime conditions, were selected to reduce manifestations of the $ClONO_2$ diurnal cycle. The theoretical precision from Table 3, the measured precision, and the average algorithmic error estimates at 32°N for April 1, 1993, are shown in Figure 5. It appears that measured and theoretical precision agree quite well with each other and both agree with the algorithmic error bar at pressures above about 30 mbar. At lower pressures (30–4.6 mbar) the algorithmic and theoretical error estimates are larger than the measured precision, indicating the possible overestimate of an error source.

Although the aerosol loading of the atmosphere varied considerably over the course of the mission [*Roche et al.*, 1994], the measured precision at 32°N or °S remained fairly constant. This finding is in line with CLAES aerosol measurements, showing that on the average the limb at this latitude remained sufficiently transparent throughout the mission not to seriously interfere with the $ClONO_2$ retrieval.

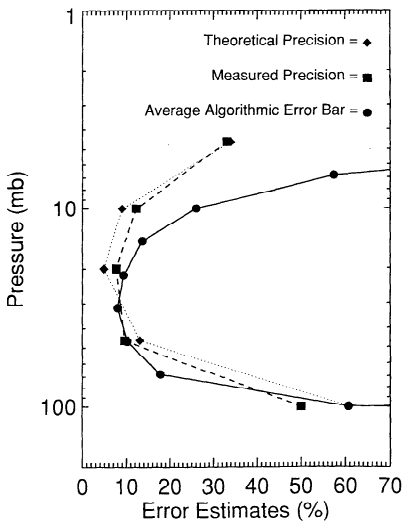

Figure 5. Precision estimates: theoretical precision, measured precision, and CLAES version 7 algorithmic error bars. All numbers pertain to midlatitude observations.

Comparisons With the LLNL-2D Model

The primary production reaction for $ClONO_2$ is the three-body recombination of chlorine monoxide and nitrogen dioxide given by

$$ClO + NO_2 + M \rightarrow ClONO_2 + M. \quad (1)$$

Chlorine nitrate is destroyed by photolysis:

$$ClONO_2 + h\nu \rightarrow Cl + NO_3 \text{ or } ClONO + O. \quad (2)$$

Daytime photolysis is sufficiently rapid to lead to a diurnal cycle. The cycle is increasingly pronounced with higher altitude as a result of a decreased rate of recombination. There is also an annual cycle as photolysis rates change with latitude and season.

This behavior is simulated in the LLNL two-dimensional atmospheric chemistry model which is described by *Patten et al.* [1994] and references included therein. Comparisons with this model were made to show how CLAES measurements conform to "state-of-the-art" theoretical expectations. Two disadvantages of these comparisons are that two-dimensional models are limited to the zonal average, and in the case of $ClONO_2$ the model results have been subject to little direct verification due to the lack of measurements.

One can construct a daily zonal mean VMR vertical profile at a given latitude from about 15 orbits with data narrowly distributed about a mean LST. For a day's sampling in a given latitude band, the LST changes by less than 20 min for ascending portions of the orbit and the same is true for the descending portions of the orbit. Figure 6 shows a multilatitude comparison of CLAES zonal mean VMR profiles with those of the LLNL-2D model during a south-looking day on April 15, 1993. Curves with open symbols (circles for CLAES, squares for LLNL) pertain to the ascending half of the CLAES orbit and open symbols to the descending half of the orbit. The legend on each plot has two columns of numbers separately describing ascending and descending observations. It contains the LST and the mean solar zenith angle (SZA) pertaining to each zonal mean. The CLAES data were filtered by rejecting data which fell outside of a 2σ statistic to eliminate occasional large spikes.

The comparison shows that the model usually agrees fairly well with CLAES up to about 30 mbar, but at higher altitudes produces significantly higher VMRs. This is true except at the southernmost comparison, 80°S, in which the measured VMRs (1) significantly exceed the model below 30 mbar, (2) are significantly less than the model from 20 to 7 mbar, and (3) are in fair agreement at around 5 mbar. Results from the previous April are very similar.

A range of LST which nearly spans the full diurnal cycle are sampled in the high and midlatitudes during a yaw period of approximately 36 days. Figure 7 compares the diurnal cycle constructed from both measured and modeled zonally averaged VMRs from the entire south-looking yaw period from March 26, 1992, to April 29, 1992. The corresponding solar zenith angles for the measurements are plotted at the bottom of the figure. Comparisons are made near 10, 22, and 46 mbar for 48°S since nearly a complete diurnal cycle is sampled over the yaw period. The measurements for LST < 12 hours were made during the ascending half of the UARS orbit, while the LST > 12 hours were made during the descending half. At 10 mbar the LLNL model shows a large depression in VMR centered near noon that is also clearly evident in the CLAES data. However, the model estimates about twice the CLAES measurement for nighttime conditions. We will return to this point after an examination of the correlative data. At 22 mbar the model and measurements agree quite well in magnitude (within about 15%) and diurnal change. At 46 mbar the measurements indicate 30–40% more $ClONO_2$ than the model, while the shallow daytime depletion is in line with model results.

One notable difference between the modeled diurnal cycle and that constructed from CLAES measurements is evident in

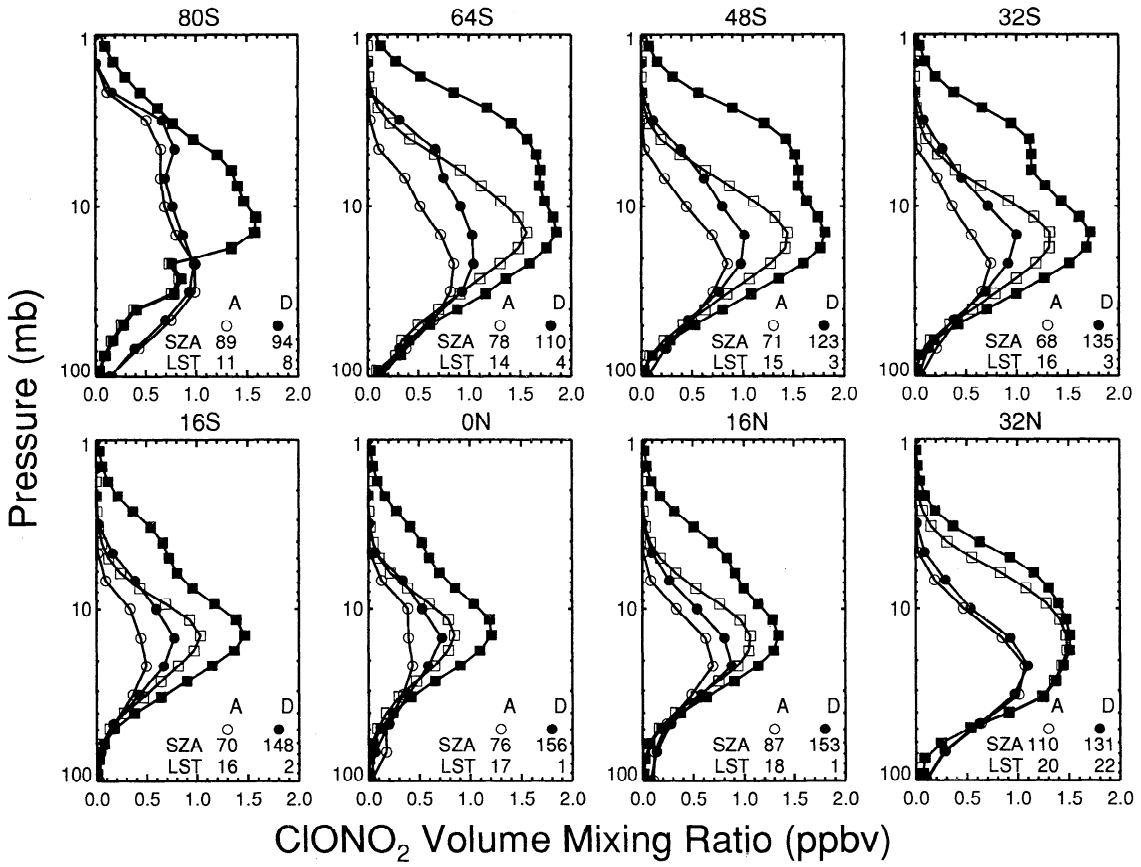

Figure 6. Zonal mean $ClONO_2$ VMR profiles from CLAES and the LLNL-2D model are shown for eight latitude bands for April 15, 1993. Four curves are shown in each panel corresponding to two CLAES zonal mean VMR profiles and respective model comparisons. Measurements acquired on descending and ascending halves of the UARS orbit (solid and open circles, respectively) are plotted separately to isolate results in local solar time and compared to LLNL-2D model (solid and open boxes, respectively).

the 22-mbar results. The early morning measurements (LST < 6 hours) acquired on the ascending half of the orbit are systematically higher by about 0.2 parts per billion by volume (ppbv) than the evening measurements (LST > 18 hours) acquired on the descending half of the orbit. One would expect them to be equal according to the model. It should be kept in mind that the observations occur over the period of a month during which time atmospheric conditions may change significantly. However predawn (LST = 6 hours) and postsunset (LST = 18 hours) measurements were both obtained on April 11, and these measurements appear to be consistent with the other morning and evening measurements, respectively, indicating a small difference between ascending and descending measurements for this particular example. The origin of this difference is not known, although line-of-sight gradients or small differences in altitude registration are possibilities. Nevertheless, this type of direct comparison of model and CLAES shows good agreement in the shape of the diurnal variation curve and was not previously available, because this is the first and only data set that covers a substantial portion of the $ClONO_2$ diurnal cycle. This figure also shows the day-to-day repeatability of CLAES zonal mean profiles, which, for these levels, appears again to be within about 0.1 ppbv.

Correlative Comparisons

While CLAES was operational, data for approximately 60 $ClONO_2$ profiles and many column measurements were collected by other instruments. This work emphasizes profile comparisons and uses all available correlative data that overlap in time and space. We also compare with column measurements from the Arctic, a region of great interest where there were very few profile measurements. The correlative data gathered for this paper come from four FTS instruments that are listed in Table 4. The majority of $ClONO_2$ profile measurements were from the Atmospheric Laboratory for Applications and Science (ATLAS 1) [*Rinsland et al.*, 1994] and ATLAS 2 [*Gunson et al.*, 1994] shuttle deployments of ATMOS. Other correlative data come from FTSs flown on balloons by D. G. Murcray et al. of the University of Denver (DU), G. C. Toon et al. of the Jet Propulsion Laboratory (JPL) and *von Clarmann et al.* [1994] of the University of Karlsruhe, Germany. The DU and JPL instruments were operated in the solar occultation mode, while MIPAS-B, the German instrument, measured thermal emission. The available correlative profile measurements sample a very limited range of latitudes, seasons, and times of day. Several column measurements using solar occultation have been published from the European Arctic Stratospheric Ozone Experiment (EASOE) and, very recently, from the Second Arctic Aircraft Stratospheric Experiment (AASE II). Some comparisons with these experiments are also included below.

The Atmospheric Trace Molecule Spectroscopy (ATMOS) Experiment, a shuttle investigation, is a fast scanning high-resolution (0.01 cm^{-1}, unapodized) Michelson interferometer

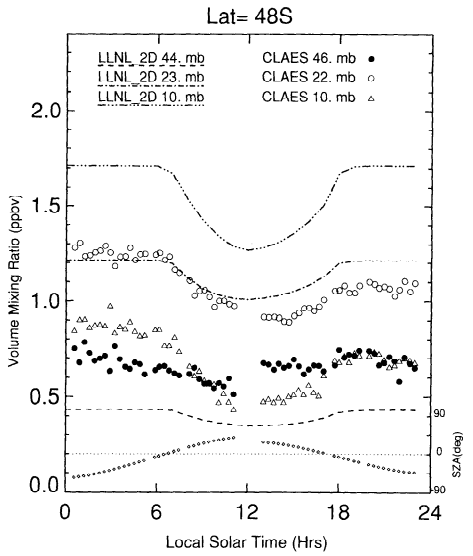

Figure 7. $ClONO_2$ diurnal cycle constructed from filtered CLAES zonal mean profiles compared with LLNL-2D results for 10, 22 and 46 mbar. The CLAES data were taken over the period from March 26 to April 29, 1992.

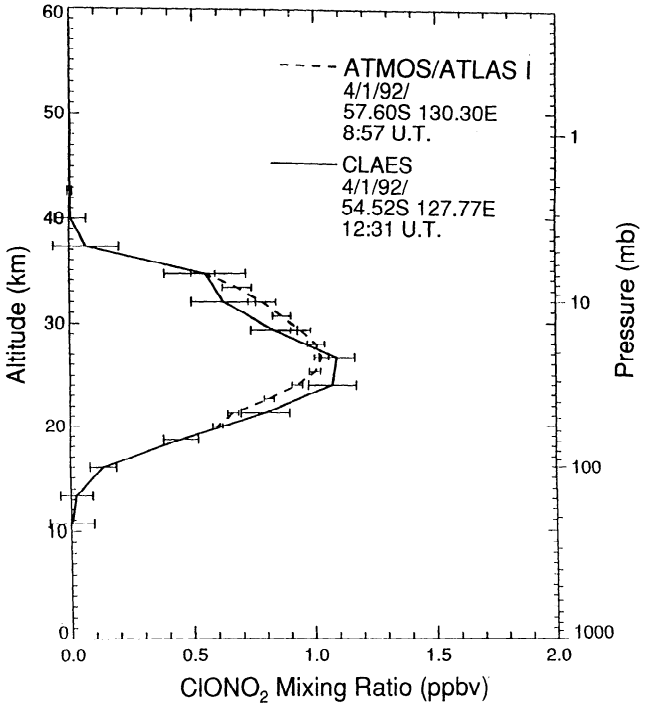

Figure 8. An example of a midlatitude CLAES/ATMOS-ATLAS 1 correlative $ClONO_2$ VMR vertical profile pair.

that records solar occultation spectra in the 2- to 16-μm region from Earth orbit. Series of high-resolution spectra of the Sun at tangent height separation of 2–3 km through and above the atmosphere were recorded at sunrise and sunset. ATMOS retrievals include N_2O, CH_4, HNO_3, $ClONO_2$, N_2O_5, CF_2Cl_2, and other species. A detailed description of the ATMOS experiment and the measurements obtained during the Spacelab 3 shuttle mission have been given by *Farmer* [1987] and *Farmer et al.* [1987b]. The ATLAS 1 flight took place from March 24 to April 7, 1992, during moderately heavy stratospheric aerosol loading from the Mount Pinatubo eruption of June 15, 1991. The coincidence criterion for comparisons of ATMOS ATLAS 1 and CLAES was maximum differences of 2° latitude, 10° of latitude equivalent longitude and 12 hours. This resulted in 14 CLAES profiles paired with ATLAS 1 sunset profiles in the southern midlatitudes and 9 CLAES profiles paired with ATLAS 1 sunrise profiles in the tropics.

Figure 8 shows an example comparison of CLAES and ATMOS ATLAS 1 midlatitude profiles with error bars for both. The CLAES data are always reported over the full altitude range observed by the instrument (nominally 10–60 km). The ATMOS experiment reports retrieval results only in an altitude regime where the data are of a prescribed high quality, which at times limits the ATMOS profiles to a smaller altitude range than the CLAES data. In this figure the ATMOS data are reported on a range from 20 to 36 km. This comparison shows agreement in both peak location and VMR magnitude with near overlap in error bars.

Figure 9 shows 9 of the 14 midlatitude sunset comparisons over the altitude range where ATMOS data are available. Each panel contains the CLAES and ATMOS profile and their difference. Also shown is the result where the CLAES measurement has been adjusted to approximately the ATMOS local solar time. When comparing CLAES and ATMOS measurements for a particular latitude but differing LSTs, the CLAES measurement was multiplied by the ratio of LLNL-2D model concentrations for the two sampling times to create an LST corrected profile. An important reason for showing many profile pairings is to illustrate the variability of $ClONO_2$ VMR profiles. All of the profiles seen in Figure 9 are from near 50°S latitude.

Most of the profiles agree well in peak height and shape. On the other hand, a few profile comparisons such as Figures 9f and 9i show quite different profile shapes. This may be due to differences in atmospheric conditions due to time and location differences.

Figures 10a and 10b show the mean and relative differences for all 14 comparisons. The mean difference is less than about 0.1 ppbv from 70 to 10 mbar and the relative difference is less than 20% in this pressure range. In the region above 10 mbar the ATMOS measurements are larger than the CLAES measurements. This difference is increased if the correction for LST differences is applied to the CLAES data. A tendency to be lower than correlative data also appears in comparisons with the DU instrument and the MkIV instruments. The source of some of this difference with ATMOS is the tendency for ATMOS profiles to curve upward at the very top of the measurement range and to curve downward more than CLAES at the low-altitude end of the measurement range

Table 4. Sources of Correlative $ClONO_2$ VMR Profile Data

Correlative Data			
Instrument	Investigator	Obser Mode	Platform
ATMOS/ATLAS 1	M. R. Gunson	solar occultation	shuttle
ATMOS/ATLAS 2	M. R. Gunson	solar occultation	shuttle
Bomem	D. G. Murcray	solar occultation	balloon
Mark IV	G. C. Toon	solar occultation	balloon
MIPAS-B	von Clarmann	emission	balloon

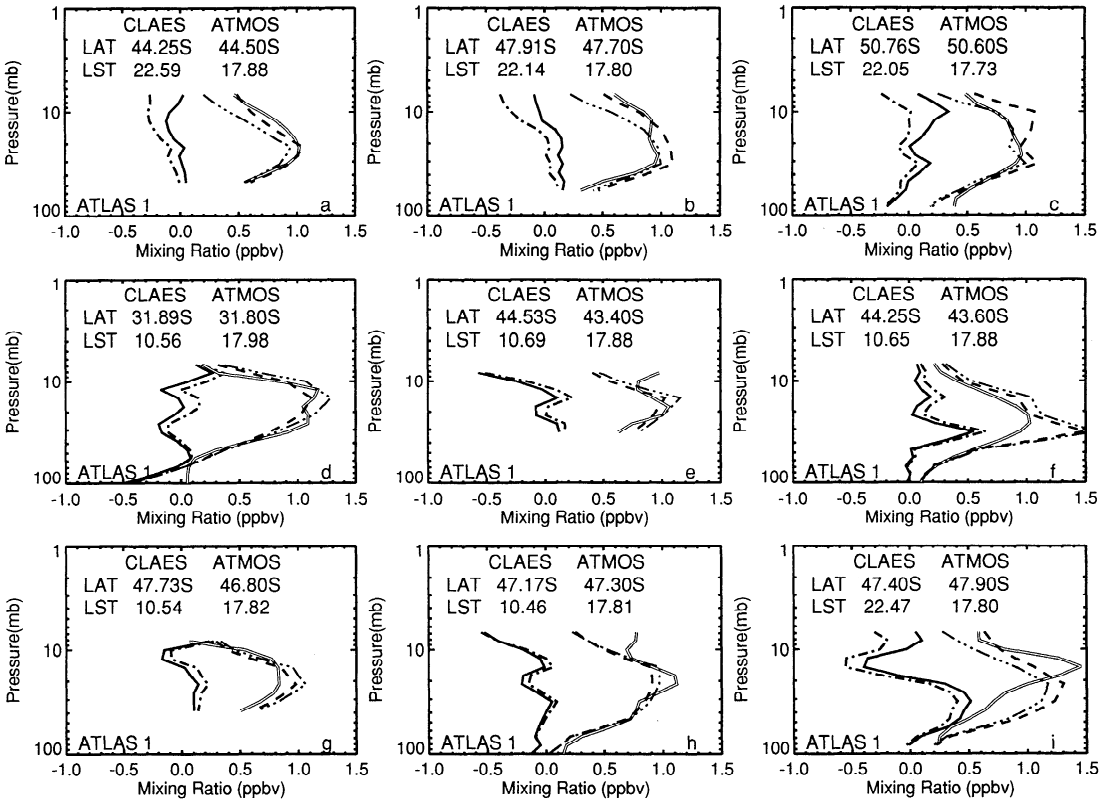

Figure 9. (a–i) Nine of 14 midlatitude $ClONO_2$ VMR vertical profile correlative pairs from CLAES and the ATMOS-ATLAS 1 mission are shown. Five curves are displayed in each panel, the ATMOS VMR profile (double line), the CLAES profile as measured (dashed), the CLAES profile adjusted for ATMOS/CLAES LST differences (dashed-three-dotted line), the VMR difference (CLAES-ATMOS) (solid), and the corrected CLAES-ATMOS VMR (dashed-dotted). The latitude and local solar time of each pair is given in the panel.

(e.g., Figures 9e, 9h, and 9i). It is noteworthy that both CLAES and ATMOS measurements, which agree fairly well at 10 mbar (within about 0.1 ppbv on the average) for these midlatitude sunset comparisons, show about 50% or ≈0.9 ppbv less $ClONO_2$ than the LLNL model calculations shown in Figure 6. The LLNL model uses the kinetic and spectral parameters recommended by the NASA Panel for Data Evaluation [*Demore et al.*, 1992]. In this evaluation and the subsequent report [*Demore et al.*, 1994] the possibility is mentioned of a nonzero yield of HCl from the reaction of ClO with OH. This reaction was not included in the present calculations. Its effect, if included, would be to reduce the calculated ClO abundance and, consequently, reduce the $ClONO_2$ abundance.

Figure 11 shows a typical comparison of a CLAES profile with one of the nine available ATMOS ATLAS 1 tropical profiles with error bars for both. The ATMOS profile is limited in altitude coverage since the Mount Pinatubo aerosol cloud prevented the near-infrared Sun sensor from acquiring the rising Sun at altitudes below about 27 km. Note that the ATMOS profile peaks near 10 mbar, while the CLAES profile peak is below 20 mbar. The lower CLAES peak appears to be an artifact discussed earlier associated with the Mount Pinatubo aerosol. We will return to this point after an examination of the ATLAS 2 tropical comparisons from a year later when there is much less aerosol.

Figures 12a and 12b show the absolute and relative mean difference of the tropical comparisons. Over the limited range where the profiles overlap, the differences are not large, ≤0.2 ppbv from about 6–18 mbar with standard deviation brackets of less than 0.3 ppbv. The relative difference, Figure 12b, for the tropical comparisons is less than 30% in this range. The correction for LST effects makes little difference because many of the CLAES measurements were at night or early morning and little adjustment is needed to compare with sunrise measurements.

ATMOS ATLAS 2

The ATMOS ATLAS 2 comparison data were acquired at sunset between April 8 and 17, 1993, in the southern tropics and midlatitudes. To obtain an adequate number of comparisons, the maximum time difference between paired profiles was increased to 24 hours. ATMOS sunrise measurements were made at high northern latitudes during this period and did not overlap the CLAES south-looking sampling region.

Figure 13 depicts six of the seven comparisons with and without correction for LST effects. Figures 13c, 13e, and 13f show very good agreement both in the absolute magnitude and in the peak positions except for points above 10 mbar in the case of Figure 13f. It is interesting to compare Figures 13c, 13e, and 13f with the ATLAS 1 tropical comparisons. These ATLAS 2 data appear to corroborate the ATLAS 1 results in that fairly sharp peaks are observed between 10 and 20 mbar. For the tropical ATLAS 2 comparisons, CLAES data tend to agree better with ATMOS in peak shape, magnitude, and altitude. This provides some evidence that the heavier aerosol loading of the ATLAS 1 period degraded the CLAES retrieval. Figure

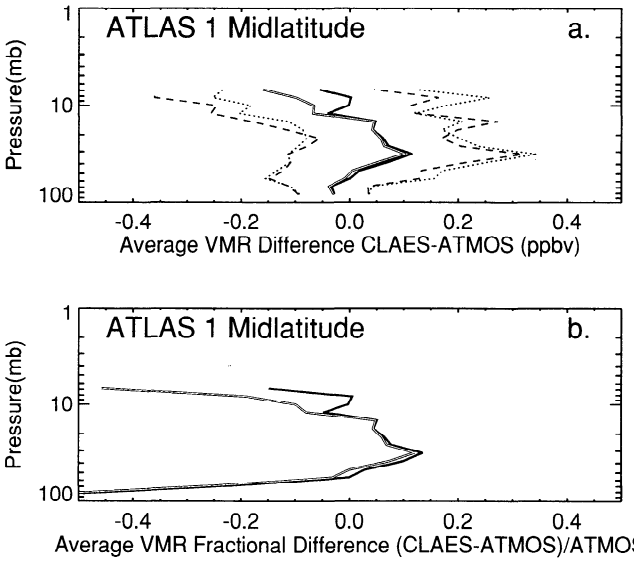

Figure 10. (a) The mean and standard deviation of the CLAES/ATMOS ATLAS 1 midlatitude profiles. The mean difference between ATMOS and CLAES data not adjusted for LST (solid line), the mean difference with CLAES LST adjustments (double line), and respective standard deviations (dotted) and (dashed) are displayed. (b) The fractional VMR differences ((CLAES-ATMOS)/ATMOS) are shown, (solid) without LST adjustments, (double line) with adjustments.

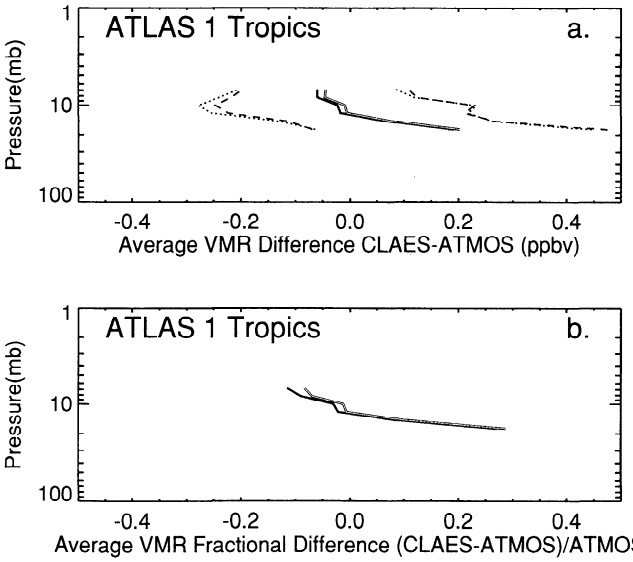

Figure 12. (a) The mean and standard deviation of the CLAES/ATMOS $ClONO_2$ tropical VMR profiles. (b) The fractional VMR differences ((CLAES-ATMOS)/ATMOS) are shown. Labeling is the same as in Figure 10.

13a has a similar shape for both profiles, but the two appear to be offset from one another. In Figures 13b and 13d the limited altitude range ATMOS and CLAES profiles show significant differences, particularly at high altitude.

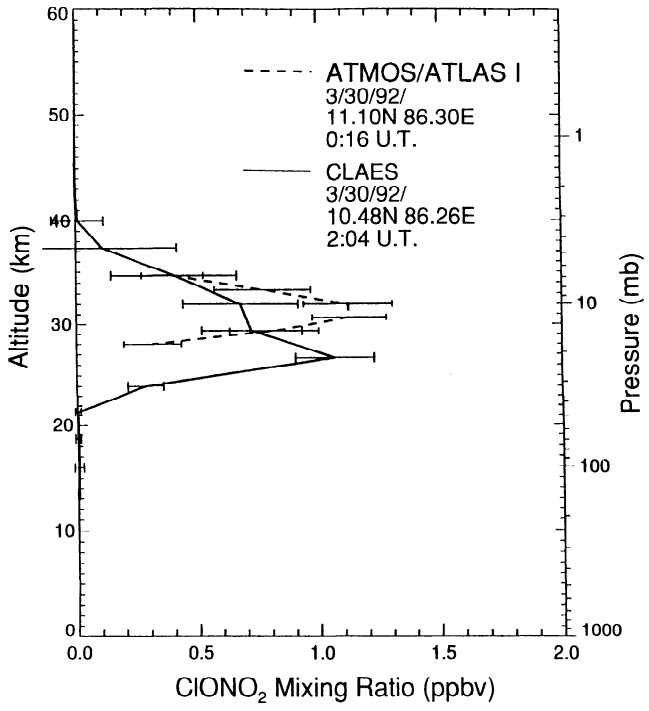

Figure 11. An example of a CLAES/ATMOS 1 comparison from the tropics showing a difference in shape which is evidently associated with high-stratospheric aerosol loading from the Mount Pinatubo eruption.

Figures 14a and 14b show a statistical summary of the ATMOS/ATLAS 2 comparisons. The most notable feature is the high-altitude falloff of the LST corrected CLAES-ATMOS mean VMR difference. This is a similar but larger high-altitude difference than appeared in the ATLAS 1 comparisons. This feature is heavily influenced by disagreement in the two pairings seen in Figures 13b and 13d. Again however, the absolute difference is less than about 0.2 ppbv from 8 to 100 mbar and less than 0.1 ppbv from 20 to 100 mbar for the "corrected" comparison. From 46 to 15 mbar the mean relative difference is less than 15% for the LST "corrected" data in Figure 14b. At the bottom of the profile where the $ClONO_2$ VMR is very low, the relative difference grows, approaching 50%.

Other Midlatitude Comparisons

The solar occultation instrument used in the balloon flights by the University of Denver group is a modified Bomem model DA3.002 Fourier transform spectrometer with a maximum optical path difference of 250 cm, which corresponds to spectral resolution (FWHM of the instrument response function) of 0.0024 cm^{-1} [*Goldman et al.*, 1992] and [*Murcray et al.*, 1990]. A liquid nitrogen-cooled HgCdTe detector was employed that covered the useful band-pass region of approximately 750–1280 cm^{-1}. Infrared absorption spectra collected during the balloon flight on July 24–25, 1992, launched from Palestine, Texas (31.6°N, 259.5°E), yielded measurements of HNO_3, $ClONO_2$, and N_2O. The sunset flight out of Barstow (Daggett Airport), California (35.4°N, 253.7°E), on April 7–8, 1993, yielded HNO_3 and $ClONO_2$ among other species. Both flights covered the altitude range of about 15 to 40 km. The University of Denver Bomem midlatitude measurement of July 24, 1992, is shown in Figure 15. In the region of the mixing ratio peak the error bars overlap. Although in the region where the CLAES error bars are relatively small ($P > 10$ mbar), the DU profile appears to be registered about 2 km higher altitude, leading to large fractional differences at low altitude. This

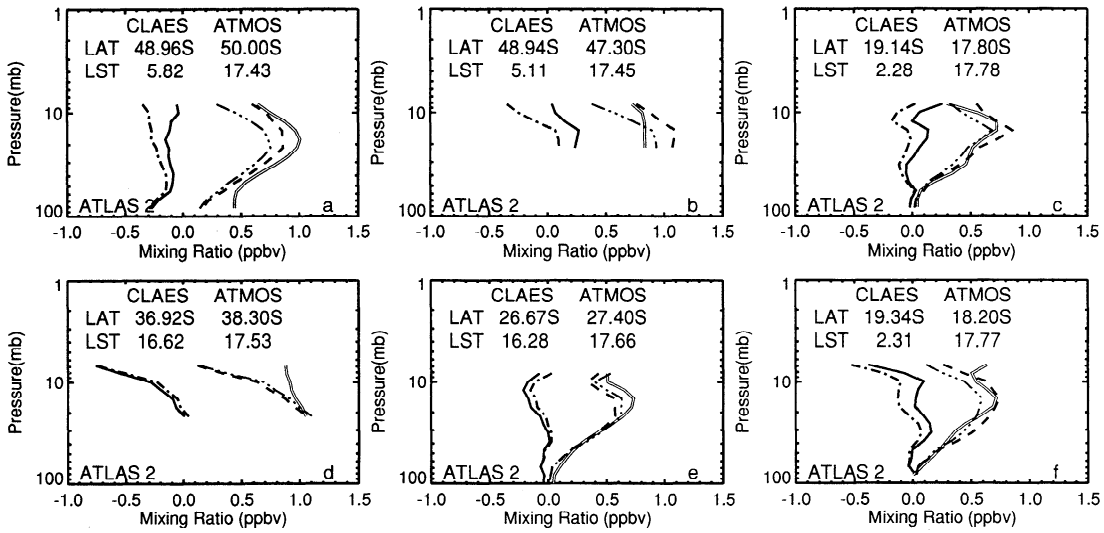

Figure 13. (a–f) Six of seven midlatitude $ClONO_2$ VMR vertical profile correlative pairs from CLAES and the ATMOS-ATLAS 2 mission are shown. Labeling is the same as in Figure 9.

difference could be due to altitude registration differences or variations in the $ClONO_2$ distribution with time and space.

Figure 16 shows another CLAES versus Bomem comparison for April 7, 1993. This comparison shows better agreement than in Figure 15. The fractional difference is generally less than 25% except at the very top and bottom of the profile.

Figures 17, 18, and 19 show comparisons of CLAES data for two flights of the JPL MkIV interferometer. This instrument is described in detail by [*Toon*, 1991]. It is a high-resolution solar absorption spectrometer which measures the entire 650 to 5650 cm^{-1} region simultaneously at a resolution of 0.01 cm^{-1}. From balloon the MkIV is capable of obtaining VMR vertical profiles between cloud top and balloon altitude (typically 37 km) for a number of atmospheric constituents. Data from two flights of this instrument on September 14–15, 1992, from Fort Sumner, New Mexico (35.2°N, 249.8°E), and another on April 4, 1993, from Barstow (Daggett Airport), California (34.8°N, 244.5°E), were available for this validation.

Figures 17, 18, and 19 show CLAES/MkIV profile comparisons for sunset and sunrise on September 14 and 15, 1992, and for sunset on April 3, 1993, respectively. During these periods, CLAES was looking south, so the JPL observations were just at the northern terminus of its observation range. Under these circumstances, CLAES samples in a very narrow range of LSTs. On these dates, CLAES viewed the midlatitudes after sunset when the $ClONO_2$ VMR is at maximum.

In all three comparisons the CLAES peak VMR appears 1 to 2 km lower than the MKIV peak and the CLAES peak VMR is less than the JPL peak even when the CLAES nighttime measurement is compared with the sunset MkIV mea-

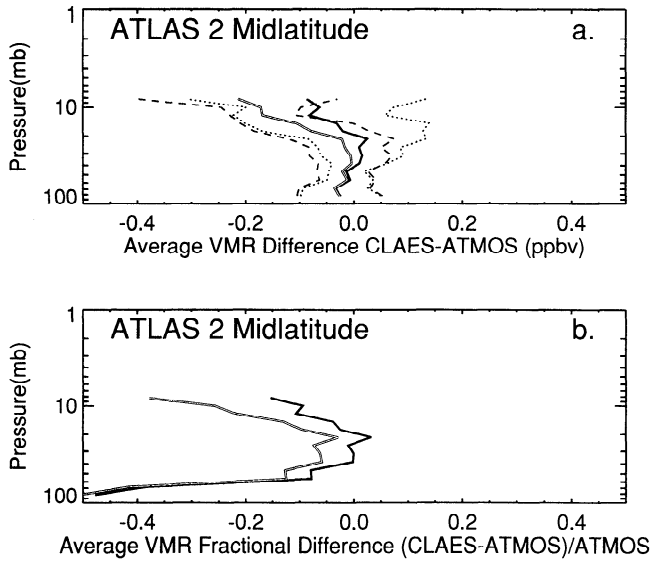

Figure 14. (a) The mean and standard deviation of the CLAES/ATMOS ATLAS 2 profiles shown in Figure 13. (b) The fractional VMR differences ((CLAES-ATMOS)/ATMOS) are shown. Labeling is the same as in Figure 12.

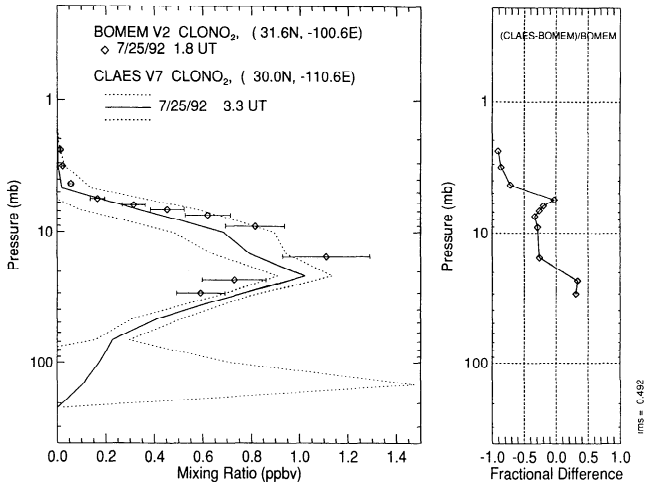

Figure 15. Correlative $ClONO_2$ VMR vertical profile pair from CLAES and the DU Bomem balloon-borne Fourier transform spectrometer (FTS) from July 25, 1992. Relative differences are shown in the right-hand panel. Denver University (DU) measurements are shown as diamonds with error bars. The CLAES measurement is shown as the solid line and the error envelope is demarked by dotted lines.

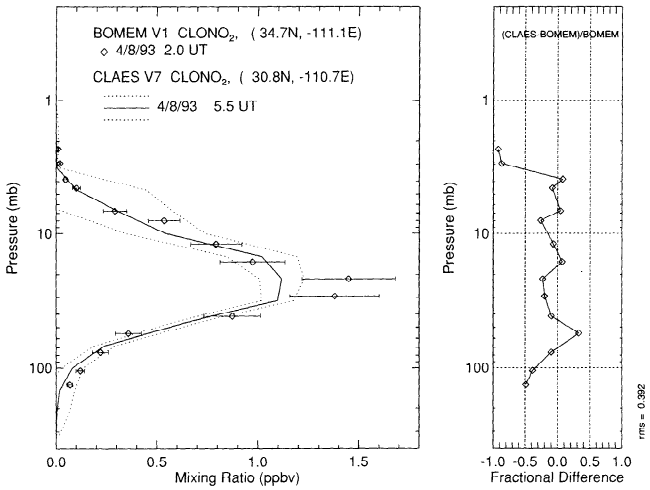

Figure 16. Correlative $ClONO_2$ VMR vertical profile pair from CLAES and the sunset measurement by the DU Bomem balloon-borne FTS from April 8, 1993.

surements, (Figures 17 and 19). The most suitable comparison in terms of LST difference is the CLAES postsunset profile comparison with the JPL September 15, 1992, sunrise profile shown in Figure 18 where peak VMRs differ by less than 25% on the altitude range from 22 to 30 km.

It is perhaps interesting to note that the 1993 MkIV and DU measurements were made within 3 days and nearly the same latitude and both were sunset measurements (Figures 16 and 19). Their VMR peaks of ≈1.35 and 1.45 ppbv at 20 mbar show good consistency between these correlative instruments.

MIPAS and Other Arctic Measurements

Comparisons with a MIPAS-B FTS thermal emission measurements of *von Clarmann et al.* [1993] are shown in Figures 20 and 21. In the first comparison the MIPAS measurement was made from a balloon launched from Kiruna, Sweden, in the early morning hours of January 13, 1992, and measurements were made within the polar vortex. CLAES was in a calibration mode at this time, but data from this locale on the previous night show the CLAES VMR profile peak 3–4 km lower and nearly equal in maximum VMR.

The second MIPAS-B/CLAES comparison from March 15, 1992, at Kiruna, Figure 21, has much closer time and space coincidence. This measurement was north of the edge of the vortex. The CLAES temperature profile agrees well with the published MIPAS temperature profile in the region up to about 10 mbar, so the comparisons which are registered in pressure are at the same potential temperatures in the lower stratosphere. The two profiles appear very similar, but the peak of the MIPAS profile appears to be lower than the CLAES profile peak by about 2 km. The VMR magnitude agrees fairly well with the error bars of the two measurements overlapping or nearly overlapping for the entire profile. Both measurements show large VMRs as one would expect in the high-latitude northern latitude winter. The column density computed from the CLAES and MIPAS-B measurements are ($3.6 \pm 0.6 \times 10^{15}$ molecules/cm^2) and (5.0×10^{15} molecules/cm^2 above 13.4 km), respectively. The column difference is due primarily to the difference of the $ClONO_2$ profile peak.

There were aircraft and ground-based column measurements on March 14 taken at locations near Estrange, Sweden (68°N, 21°E), as part of EASOE and AASE II programs. The ground-based measurements show a $ClONO_2$ column of (6.9×10^{15} molecules/cm^2 ± 27%) [*Adrian et al.*, 1994]. Aircraft-based measurements of *Toon et al.* [1992] over Estrange yield columns of ($4.6 \pm .5$) $\times 10^{15}$ molecules/cm^2. These can be compared with two CLAES partial columns of 3.5 ± 0.4 and $3.7 \pm 0.6 \times 10^{15}$ molecules/cm^2, within 10° longitude and 2° latitude of Estrange. The column error estimates are the $ClONO_2$ number density weighted rss of CLAES error bars.

A CLAES profile from this comparison is shown in Figure 22 where the VMR profile, the number density profile, and the

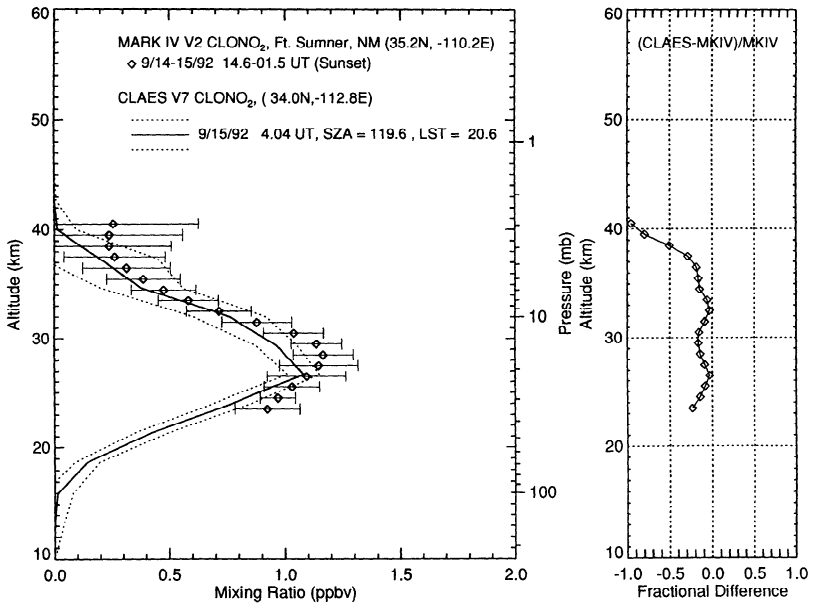

Figure 17. Correlative $ClONO_2$ VMR vertical profile pair from CLAES and a sunset measurement by the Jet Propulsion Laboratory (JPL) Mark IV (MkIV) balloon-borne FTS from September 15, 1992. Right-hand panel displays the fractional difference between the two measurements.

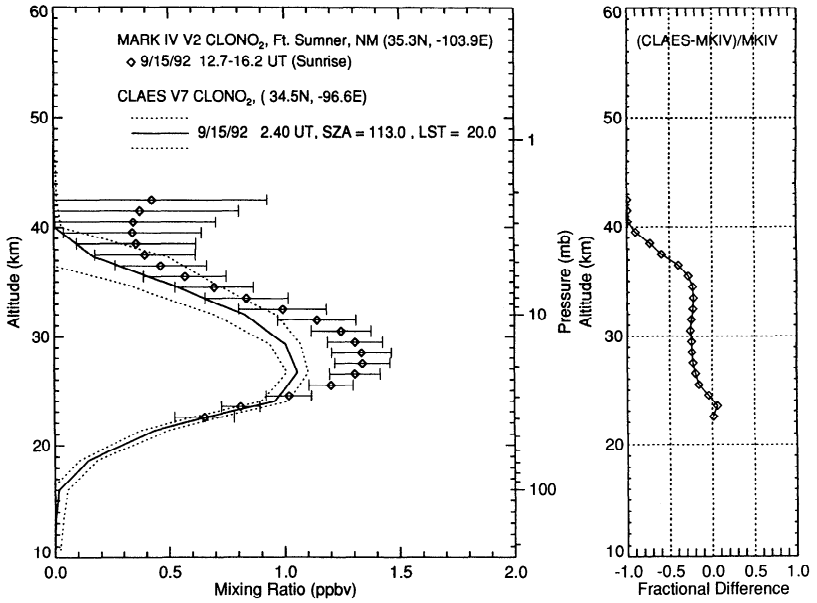

Figure 18. Correlative $ClONO_2$ VMR vertical profile pair from CLAES and a sunrise measurement by the JPL MkIV balloon-borne FTS from September 15, 1992. Right-hand panel displays the fractional difference between the two measurements.

integrated column are displayed. In these polar comparisons a significant portion of the number density profile is frequently below the CLAES measurement range. The integration of this truncated column gives a low bias to the CLAES column estimate. Incidently, at lower latitudes the CLAES detector array does not appear to cut off a significant part of the column and is more suitable for column comparisons.

Within the sources of uncertainty such as atmospheric spatial variability, time coincidence, measurement precision, and profile truncation by CLAES, the column comparisons show that all instruments were measuring high $ClONO_2$ columns, characteristic of the polar winter, and all are in reasonable quantitative agreement (within 30–40%).

Correlative Comparison Summary

This exercise taken as a whole shows that CLAES agrees with the correlative measurements to within about 25% from 10 to 50 mbar, in the neighborhood of the peak of the $ClONO_2$ VMR profile in the midlatitudes. Above this region ($P < 10$ mbar), nearly all comparisons show CLAES to be increasingly negatively biased with altitude. The large systematic differences seen at high altitude (above 8 mbar) are expected on the

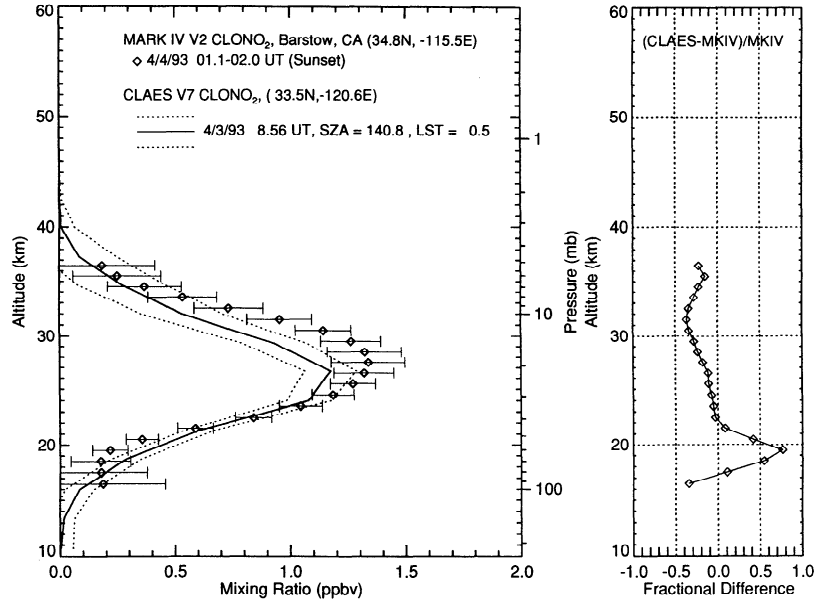

Figure 19. Correlative $ClONO_2$ VMR vertical profile pair from CLAES and a sunset measurement by the JPL MkIV balloon-borne FTS from April 4, 1993. Right-hand panel displays the fractional difference between the two measurements.

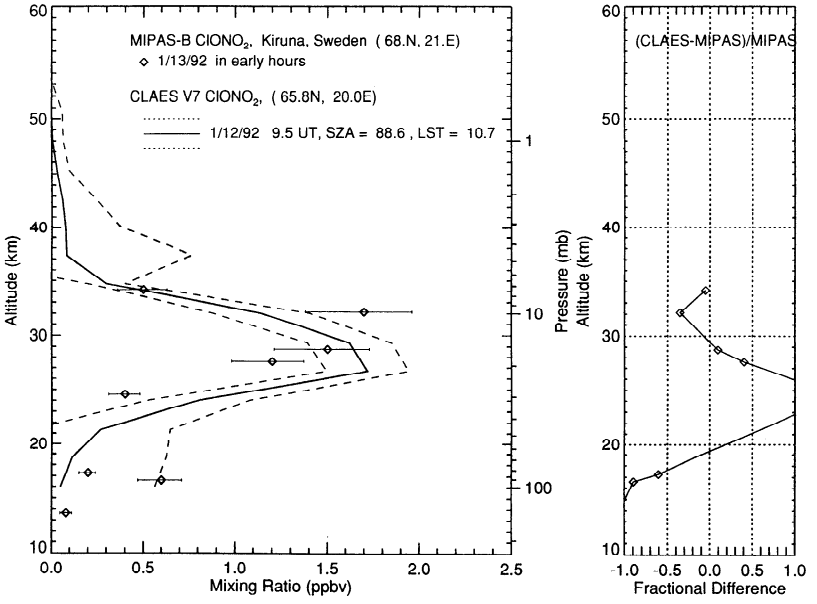

Figure 20. Correlative $ClONO_2$ VMR vertical profile pair from CLAES (sunset January 12, 1992) and a nighttime measurement by MIPAS-B on January 13, 1992. Right-hand panel displays the fractional difference between the two measurements.

basis of our systematic error analysis in Table 2. Below about 50 mbar in the region of steep vertical gradient and low VMRs the majority of the comparisons show CLAES to be biased increasingly low with decreasing altitude. The altitudes of greatest disagreement correspond to regions where the precision of the CLAES is relatively poor; see Table 3. The ATLAS 1 tropical data covered a very limited altitude range. CLAES comparisons show little relative mean difference at 10 mbar (>5%) but an increasing positive mean difference (20%) at lower altitudes (20 mbar), which adds additional evidence of aerosol interference in the tropics in the early part of the mission. Arctic comparisons with MIPAS-B and column measurements corroborate high $ClONO_2$ concentrations observed by CLAES in March 1992. The MIPAS-B measurements also show reasonable agreement in VMR profiles given the variability of the atmosphere near the Arctic vortex.

Known Artifacts

There are some known artifacts in the data that will be addressed here. These include (1) occasional spikes due to a processing code error, (2) unrealistically high VMRs observed,

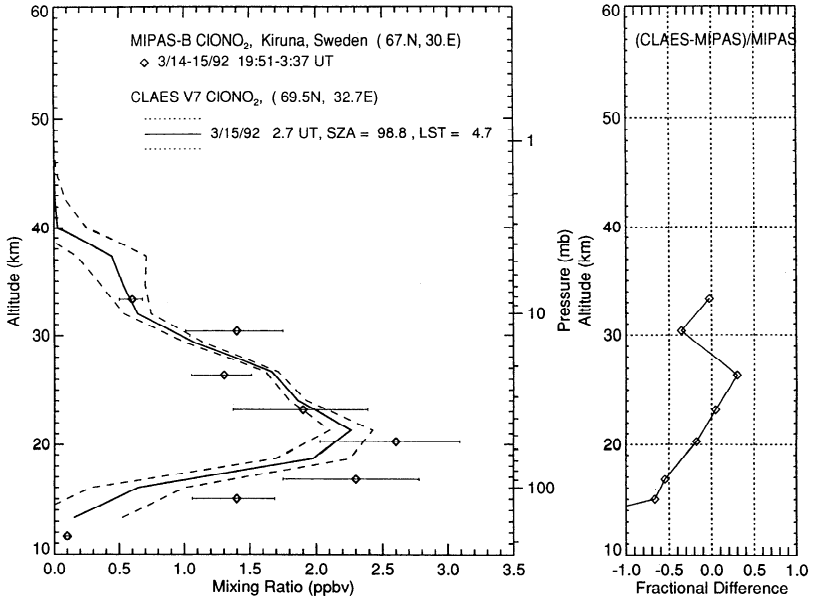

Figure 21. Correlative $ClONO_2$ VMR vertical profile pair from CLAES and a nighttime measurement by MIPAS-B from March 14–15, 1992. Right-hand panel displays the fractional difference between the two measurements.

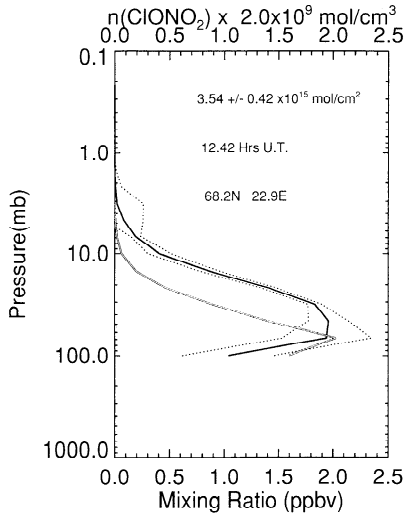

Figure 22. Four curves are shown that include the CLAES VMR vertical profile (solid line), associated upper and lower error bars (dotted lines), and a number density profile calculated from the CLAES measurement (double line). Also shown in each panel is the calculated vertical $ClONO_2$ column, the time of the profile measurement, and the location of the profile. Column comparisons with aircraft and ground-based column measurements near Estrange, Sweden, on March 14, 1992, are discussed in the text.

at times, in the neighborhood of polar stratospheric clouds (PSCs), and (3) anomalous tropical VMR profiles in the presence of high volcanic aerosol loading. Spikes are sharp, rather random, single-point maxima with small error bars, which appear occasionally in the version 7 data. The maximum inorganic chlorine in the stratosphere has been estimated at ≈3.44 ppbv [*Gunson et al.*, 1994] and, for example, on UARS day 120 (January 9, 1992), out of 1285 $ClONO_2$ profiles there were five with a datum exceeding 3.5 ppbv. Four of these spikes were traced to a coding error. The spikes generally occur on the top side of the profile at an altitude of 32–36 km and have small (<10%) error bars. The remaining spiked profile was associated with an Arctic PSC; it differed from the others in the location of the spike (22 km) and size of the error bars (>100%). In this case the spatial structure of the PSC probably caused large fitting residuals which expanded the error bars. In the Antarctic winter, excessive VMRs are also seen in the neighborhood of PSCs. These have large error bars.

Figure 23 shows an example of the second kind of artifact, a PSC coincident CLAES $ClONO_2$ retrieval along with corresponding aerosol extinction (790 cm^{-1}). Within very dense PSCs the solution has very large error bars. Excessive $ClONO_2$ VMRs (solid line) occur frequently just above the PSCs (indicated by the double line); the error bars shown, as dashed lines, expand appropriately in these cases, indicating large residuals due to spectral distortions observed on the detector just at the top of the cloud in a region of extreme vertical radiance gradient. There are also a few profiles with suspiciously high values (3.5–5 ppbv) in the Antarctic winter with error bars of 25% or less. These are also usually associated with PSCs.

Figure 24 also shows the third kind of artifact mentioned above, anomalous profiles near dense volcanic aerosol. The figure shows zonal mean cross sections of $ClONO_2$ VMR for January 9, 1992, and January 4, 1993. The volcanic aerosol cloud from Mount Pinatubo had diminished considerably between these dates. Nearly identical measurement scenarios were used to mitigate other factors such as differences in LST. The lower part of $ClONO_2$ profiles ($P > 30$ mbar) in the region from 16°N to 16°S shows a very low VMR in the winter of 1992. In this region the relatively weak $ClONO_2$ spectral feature is nearly obscured by thick aerosol.

Just above the high-aerosol loading ($10 < P < 30$ mbar) is a sharp maximum in the $ClONO_2$ profile. The peaked tropical zonal mean profile in 1992 is to be compared with the smoother 1993 profile. This exaggerated peak probably is an artifact of the kind discussed earlier under Systematic Error sources. The sharp peak in $ClONO_2$ VMR is not accompanied by large algorithmic error estimates. This feature is present in the tropical $ClONO_2$ data until July 1992. Further refinements in instrument characterization may mitigate this in future versions of the processing software.

Summary and Conclusions

An analysis of the quality of the CLAES $ClONO_2$ version 7 data from several aspects has been presented. Known random and systematic retrieval uncertainties have been discussed. Diurnal and geographical variations in the CLAES data have been compared with calculations of the LLNL-2D atmospheric chemistry model, CLAES data have been compared to correlative data from several sources, and known problems have been described. The majority of the CLAES data in the $10 < P < 50$ mbar range appears to be of good quality with average differences of less than 25% compared to correlative measurements. Theoretical and measured precision are within 15% in the range ($10 < P < 50$ mbar). Repeatability of diurnal cycle variations is apparent up to about 5 mbar, depending upon latitude. Our representation of the $ClONO_2$ diurnal cycle constructed from more the 30 days of data agrees well with the LLNL cycle. Qualitative agreement is shown between model and measurement in global distribution. However, many cases show that the amount of $ClONO_2$ calculated by the model significantly exceeds that measured by CLAES. CLAES and ATMOS measurements show relatively good midlatitude agreement suggesting that the major source of discrepancy is in

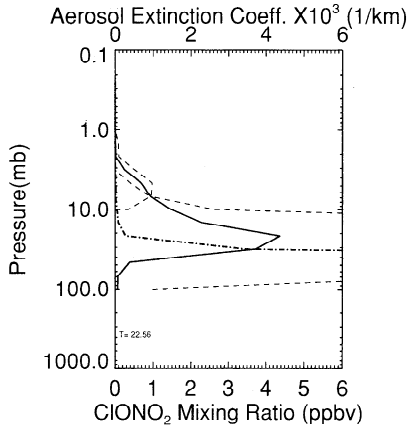

Figure 23. A profile retrieved in the presence of an Antarctic polar stratospheric cloud on August 17, 1992. The data are from 80°S, 75°W. Of particular note is the sharp peak of extremely high $ClONO_2$ VMRs (solid line) just above the region high aerosol extinction (dashed-dotted). Also note that the error bars (dashed) expand, indicating high uncertainty.

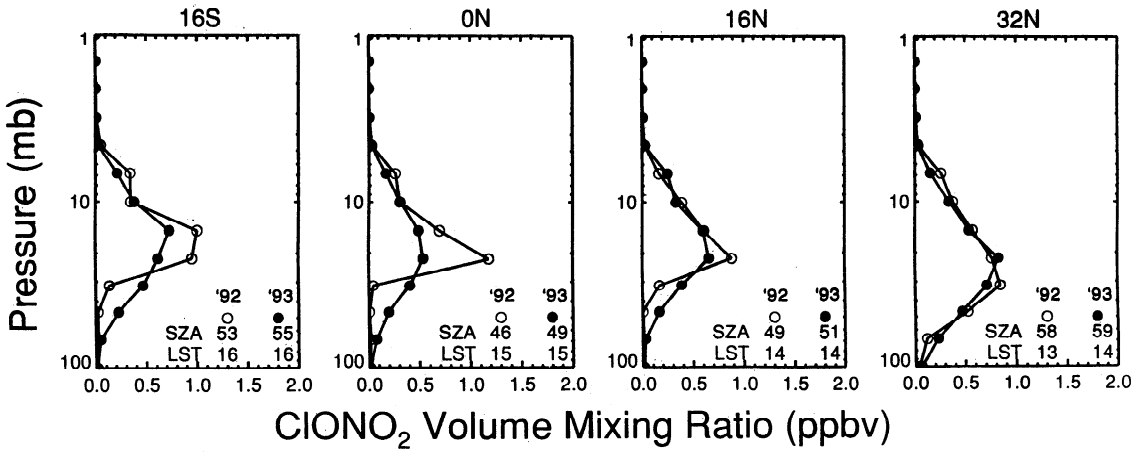

Figure 24. This figure shows a multilatitude comparison of zonal mean $ClONO_2$ VMR for January 9, 1992 (open circles) and January 4, 1993 (solid circles). Nearly identical measurement conditions have been selected for this comparison in an attempt to eliminate LST differences. Each panel is labeled with the LST of the measurement, the solar zenith angle, the mean latitude of the comparison and the number of profiles contributing to the mean. Two aspects of interference from Mount Pinatubo aerosol in the tropics (16°S–16°N) are apparent in this figure. The first is the peak at about 20 mbar in the 1992 data which does not appear in 1993 and the second is the very low 1992 values found below 30 mbar.

the model. A possible explanation in terms of a missing reaction $ClO + OH \rightarrow HCl + O_2$ is suggested.

Overall, this validation study indicates that the majority of CLAES $ClONO_2$ profile measurements are of good quality and should be very useful in quantitative and qualitative chemical studies of the stratosphere. All version 7 CLAES products are currently available on the Goddard Distributed Active Archive Center [*Rood and Geller*, 1994].

Acknowledgments. We thank our LPARL colleagues G. A. Ely, F. Zele, W. G. Uplinger, M. Ewing, and S. Claflin for their contributions. We thank L. V. Lyjak and C. A. Craig of NCAR for assistance in producing repeatability error estimates, and ATMOS comparisons, respectively. At LPARL this work was supported by the NASA UARS contract NAS5-27752, at NCAR by the NASA UARS contract S-10782-C, the MARK IV correlative measurements by the NASA UARS correlative Program, the ATMOS by personnel at the Jet Propulsion Laboratory, California Institute of Technology, under contract with the National Aeronautics and Space Administration, and the Lawrence Livermore contribution under the auspices of the U.S. Department of Energy by the Lawrence Livermore National Laboratory under contract No. W-7405-Eng-48.

References

Adrian, G. P., et al., First results of ground-based FTIR measurements of atmospheric trace gases in north Sweden and Greenland during EASOE, *Geophys. Res. Lett.*, *21*, 1343–1346, 1994.

Bailey, P. L., et al., Comparison of cryogenic limb array etalon spectrometer ozone observations with correlative measurements, *J. Geophys. Res.*, this issue.

Ballard, J., W. B. Johnston, M. R. Gunson, and P. T. Wassel, Absolute absorption coefficients of $ClONO_2$ infrared bands at stratospheric temperatures, *J. Geophys. Res.*, *93*, 1659–1665, 1988.

Clough, S. A., F. X. Kneizys, G. P. Anderson, E. P. Shettle, J. H. Chetwynd, L. W. Abreu, L. A. Hall, and R. D. Worsham, FASCOD3: Spectral simulation, in paper presented at the International Radiation Symposium on Current Problems in Atmospheric Radiation, Int. Assoc. of Meteorol. and Atmos. Phys., Lille, France, August 18–24, 1988.

Coffey, M., W. G. Mankin, and A. Goldman, Airborne measurements of stratospheric constituents over Antarctica in the austral spring 1987, 2, Halogen and nitrogen trace gases, *J. Geophys. Res.*, *94*, 16,597–16,613, 1989.

DeMore, W. B., S. P. Sander, D. M. Golden, R. F. Hampson, M. J. Kurylo, C. J. Howard, A. R. Ravishankara, C. E. Kolb, Jr, and M. J. Molina, *Chemical Kinetics and Photochemical Data for Use in Stratospheric Modeling: Evaluation 10*, Jet Propul. Lab., Calif. Inst. of Technol., Pasadena, 1992.

DeMore, W. B., S. P. Sander, D. M. Golden, R. F. Hampson, M. J. Kurylo, C. J. Howard, A. R. Ravishankara, C. E. Kolb Jr, and M. J. Molina, *Chemical Kinetics and Photochemical Data for Use in Stratospheric Modeling: Evaluation 11*, Jet Propul. Lab., Calif. Inst. of Technol., Pasadena, 1994.

Edwards, D. P., GENL2: A general line-by-line atmospheric transmittance and radiance model. Version 3.0 description and users guide, *Tech. Rep. NCAR/TN-367+STR*, Natl. Cent. for Atmos. Res., Boulder, Colo., 1992.

Farman, J. C., B. G. Gardiner, and J. D. Shanklin, Large losses of total ozone in Antarctica reveal seasonal ClO_x/NO_x interaction, *Nature*, *315*, 207–210, 1985.

Farmer, C. B., High resolution infrared spectroscopy of the Sun and Earth's atmosphere from space, *Mikrochim. Acta*, *3*, 189–214, 1987.

Farmer, C. B., G. C. Toon, P. W. Shaper, J. F. Blavier, and L. L. Lowes, Stratospheric trace gases in the spring 1986 Antarctic atmosphere, *Nature*, *329*, 126–130, 1987a.

Farmer, C. B., O. F. Raper, and F. G. O'Callaghan, Final report on the first of the ATMOS instrument during the Spacelab 3 mission, April 29 through May 6, 1985, Jet Propul. Lab., Pasadena, Calif., 1987b.

Gille, J. C., et al., Validation of temperature retrievals obtained by the limb infrared monitor of the stratosphere (LIMS) experiment on Nimbus 7, *J. Geophys. Res.*, *89*, 5147–5160, 1984.

Gille, J. C., et al., Accuracy and precision of cryogenic limb array etalon spectrometer (CLAES) temperature retrievals, *J. Geophys. Res.*, this issue.

Goldman, A., F. J. Murcray, R. D. Blatherwick, J. J. Kosters, D. G. Murcray, C. P. Rinsland, J.-M. Flaud, and C. Camy-Peyret, Stratospheric HNO_3 measurements from 0.002 cm^{-1} resolution solar occultation spectra with improved spectroscopic line parameters in the 5.8 μm region, *J. Geophys. Res.*, *97*, 2561–2567, 1992.

Goldman, A., C. P. Rinsland, F. J. Murcray, R. D. Blatherwick, and D. G. Murcray, High resolution studies of heavy NO_y molecules in atmospheric spectra, *J. Quant. Spectrosc. Radiat. Transfer*, *52*, 367–377, 1994.

Gordley, L. L., Marshall, B. T., and D. A. Chu, LINEPAK: Algorithms for modeling spectral transmittance and radiance, *J. Quant. Spectros. Radiat. Transfer*, *52*, 563–580, 1994.

Gunson, M. R., M. C. Abrams, L. L. Lowes, E. Mahieu, R. Zander, C. P. Rinsland, M. K. W. Ko, N. D. Sze, and D. K. Weisenstein, Increase in levels of stratospheric chlorine and fluorine loading between 1985 and 1992, *Geophys. Res. Lett.*, *21*, 2223–2226, 1994.

Hoffman, D. J., and S. Solomon, Ozone destruction through heterogeneous chemistry following the eruption of El Chichon, *J. Geophys. Res.*, *94*, 5029–5041, 1989.

James, T. C., A. E. Roche, B. C. Steakley, J. B. Thatcher, J. B. Kumer, L. W. Sterritt, J. F. Potter, and J. C. Dawson, Spectral Calibration of the Cryogenic Limb Array Etalon Spectrometer (CLAES), in *Optical Remote Sensing of the Atmosphere, 1990 Tech. Dig. Ser.*, vol. 4, p. 172, Opt. Soc. of Am., Incline Village, Nev., Feb. 12–15, 1990.

Kumer, J. B., J. L. Mergenthaler, T. C. James, A. E. Roche, L. W. Sterritt, and J. F. Potter, Detector channeling hypothesis for enhanced structure observed in CLAES system blocker filter functions, in *Optical Remote Sensing of the Atmosphere, 1990 Tech. Dig. Ser.*, vol. 4, p. 164, Opt. Soc. of Am., Incline Village, Nev., Feb. 12–15, 1990.

Kumer, J. B., J. L. Mergenthaler, and A. E. Roche, CLAES CH_4, N_2O, and CCl_2F_2 global data, *Geophys. Res. Lett.*, *20*, 1239–1242, 1993.

Kumer, J. B., et al., Comparison of correlative data with nitric acid data version 7 from the cryogenic limb array etalon spectrometer (CLAES) instrument deployed on the NASA Upper Atmosphere Research Satellite (UARS), *J. Geophys. Res.*, this issue.

Marshall, B. T., L. L. Gordley, and D. A. Chu, BANDPAK: Algorithms for modeling broadband transmittance and radiance, *J. Quant. Spectrosc. Radiat. Transfer*, *52*, 563–580, 1994.

Massie, S. T., et al., Atmospheric infrared emission of $ClONO_2$ observed by a balloon-borne Fourier spectrometer, *J. Geophys. Res.*, *92*, 14,806–14,814, 1987.

Massie et al., Validation studies using multiwavelength CLAES observations of stratospheric aerosol, *J. Geophys. Res.*, this issue.

Mergenthaler, J. L., J. F. Potter, J. B. Kumer, T. C. James, and A. E. Roche, Retrieval of CLAES filter shapes from spectral calibration data, in *Optical Remote Sensing of the Atmosphere, 1990 Tech. Dig. Ser.*, vol. 4, 180, Opt. Soc. of Am., Incline Village, Nev., Feb. 12–15, 1990.

Mergenthaler, J. L., J. F. Potter, J. B. Kumer, T. C. James, and A. E. Roche, Derivation of CLAES filter shapes, paper presented at Sixth Topical Meeting on Optical Remote Sensing of the Atmosphere, Opt. Soc. of Am., Salt Lake City, March 8–12, 1993.

Murcray, D. G., et al. Stratospheric distribution of $ClONO_2$, *Geophys. Res. Lett.*, *6*, 857–859, 1979.

Murcray, F. J., J. J. Kosters, R. D. Blatherwick, J. Olson, and D. G. Murcray, High resolution solar spectrometer system for measuring atmospheric constituents, *Appl. Opt.*, *29*, 1520–1525, 1990.

Patten, K. O., Jr., P. S. Connell, D. E. Kinnison, D. J. Wuebbles, T. G. Slanger, and L. Froidevaux, Effect of vibrationally exited oxygen on ozone production in the stratosphere, *J. Geophys. Res.*, *99*, 1211–1224, 1994.

Prather, M., Catastrophic loss of stratospheric ozone in dense volcanic clouds, *J. Geophys. Res.*, *97*, 10,187–10,191, 1992.

Reber, C. A., The Upper Atmosphere Research Satellite (UARS), *Geophys. Res. Lett.*, *20*, 1215–1218, 1993.

Rinsland, C. P., et al., Tentaitve identification of the 780 cm^{-1} ν_4 band Q-branch of chlorine nitrate in high resolution solar absorption spectra of the stratosphere, *J. Geophys. Res.*, *90*, 7931–7943, 1985.

Rinsland, C. P., M. R. Gunson, M. C. Abrams, R. Zander, E. Mahieu, A. Goldman, M. K. W. Ko, J. M. Rodriguez, and N. D. Sze, Profiles of stratospheric chlorine nitrate ($ClONO_2$) from atmospheric trace molecule spectroscopy/ATLAS 1 infrared solar occultation spectra, *J. Geophys. Res.*, *99*, 18,895–18,900, 1994.

Roche, A. E., J. B. Kumer, J. L. Mergenthaler, G. A. Ely, W. G. Uplinger, J. F. Potter, T. C. James, and L. W. Sterritt, The cryogenic limb array etalon spectrometer (CLAES) on UARS: Experiment description and performance, *J. Geophys. Res.*, *98*, 10,763–10,775, 1993a.

Roche, A. E., J. B. Kumer, and J. L. Mergenthaler, CLAES observations of $ClONO_2$ and HNO_3 in the Antarctic stratosphere, between June 15 and September 17, 1992, *Geophys. Res. Lett.*, *20*, 1223–1226, 1993b.

Roche, A. E., J. B. Kumer, J. L. Mergenthaler, R. W. Nightingale, W. G. Uplinger, G. A. Ely, J. F. Potter, D. J. Wuebbles, P. S. Connell, and D. E. Kinnison, Observations of lower stratospheric $ClONO_2$, HNO_3 and aerosol by the UARS CLAES experiment between January 1992 and April 1993, *J. Atmos. Sci.*, *20*, 2877–2902, 1994.

Rodgers, C., Retrieval of atmospheric temperature and composition from remote measurements of thermal radiation, *Rev. Geophys.*, *14*, 609–624, 1976.

Rodgers, C., Retrieval of atmospheric temperature and composition from remote measurements of thermal radiation, *J. Atmos. Sci.*, *20*, 2877–2902, 1994.

Rood, R., and M. Geller (Eds.), *J. Atmos. Sci.*, *20*, 2781–2782, 1994.

Rothman, L. S., et al., The HITRAN molecular database: Editions of 1991 and 1992, *J. Quant. Spectrosc. Radiat. Transfer*, *48*, 469–507, 1992.

Rowland, F. S., J. E. Spencer, and M. J. Molina, Stratospheric formation and photolysis of chlorine nitrate, *J. Phys. Chem.*, *80*, 2711–2713, 1976a.

Rowland, F. S., J. E. Spencer, and M. J. Molina, Estimated relative abundance of chlorine nitrate among stratospheric chlorine compounds, *J. Phys. Chem.*, *80*, 2713–2715, 1976b.

Solomon, S., Progress toward a quantitative understanding of Antarctic ozone depletion, *Nature*, *347*, 347–353, 1990.

Sterritt, L. W., T. C. James, J. B. Kumer, A. E. Roche, B. C. Steakley, and K. M. Zickuhr, Radiometric calibration of the cryogenic limb array etalon spectrometer (CLAES), in *Optical Remote Sensing of the Atmosphere, 1990 Tech. Dig. Ser.*, vol. 4, p. 168, Opt. Soc. of Am., 1990.

Toon, G. C., JPL Mark IV interferometer, *Opt. Phot. News*, *2*, 19–21, 1991.

Toon, G. C., C. B. Farmer, L. L. Lowes, P. W. Shaper, J. F. Blavier, and R. H. Norton, Infrared aircraft measurements of stratospheric compositions over Antarctica during September 1987, *J. Geophys. Res.*, *94*, 16,571–16,596, 1989.

Toon, G. C., J.-F. Blavier, J. N. Solario, and J. T. Szeto, Airborne observations of the 1992 Arctic winter stratosphere by FTIR solar absorption spectroscopy, *Opt. Meth. Atmos. Chem.*, *1715*, 457–467, 1992.

Toumi, R., R. L. Jones, and J. A. Pyle, Stratospheric ozone depletion by $ClONO_2$ photolysis, *Nature*, *365*, 37–39, 1993.

Von Clarmann, T., H. Fischer, F. Friedl-Vallon, A. Linden, H. Oelhaf, C. Piesch, and M. Seefeldner, Retrieval of stratospheric O_3, HNO_3, and $ClONO_2$ profiles from 1992 MIPAS-B limb emission spectra: Method, results, and error analysis, *J. Geophys. Res.*, *98*, 20,495–20,506, 1993.

Zander, R., C. P. Rinsland, C. B. Farmer, L. R. Brown, and R. H. Norton, Observation of several chlorine nitrate ($ClONO_2$) bands in stratospheric infrared spectra, *Geophys. Res. Lett.*, *13*, 757–760, 1986.

M. C. Abrams, J.-F. Blavier, M. R. Gunson, B. Sen, and G. C. Toon, Jet Propulsion Laboratory, Pasadena, CA 91109.

P. L. Bailey, D. Edwards, J. C. Gille, and S. T. Massie, National Center for Atmospheric Research, Boulder, CO 80307.

P. S. Connell and D. E. Kinnison, Lawrence Livermore National Laboratory, Livermore, CA 94550.

A. Goldman, D. G. Murcray, and F. J. Murcray, Department of Physics, University of Denver, Denver, CO 80210.

J. B. Kumer, J. L. Mergenthaler (corresponding author), R. W. Nightingale, J. F. Potter, and A. E. Roche, Lockheed Palo Alto Research Laboratory, 3251 Hanover Street, Org. 91 20, Bldg. 252, Palo Alto, CA 94304.

(Received March 30, 1995; revised November 6, 1995; accepted February 2, 1996.)